University of Maribor
Faculty of Energy Technology

Journal of ENERGY TECHNOLOGY

Volume 12 / Issue 1
APRIL 2019
www.fe.um.si/en/jet.html

Journal of ENERGY TECHNOLOGY

VOLUME 12 / Issue 1

Revija Journal of Energy Technology (JET) je indeksirana v bazah INSPEC© in Proquest's Technology Research Database.

The Journal of Energy Technology (JET) is indexed and abstracted in database INSPEC© and Proquest's Technology Research Database.

JOURNAL OF ENERGY TECHNOLOGY

Tehnični urednik / TECHNICAL EDITOR

Sonja Novak

Tehnična podpora / TECHNICAL SUPPORT

Tamara BREČKO BOGOVČIČ

Izhajanje revije / PUBLISHING

Revija izhaja štirikrat letno v nakladi 100 izvodov. Članki so dostopni na spletni strani revije - www.fe.um.si/si/jet.html / The journal is published four times a year. Articles are available at the journal's home page - www.fe.um.si/en/jet.html.

Cena posameznega izvoda revije (brez DDV) / Price per issue (VAT not included in price): 50,00 EUR

Informacije o naročninah / Subscription information: http://www.fe.um.si/en/jet/subscriptions.html

Lektoriranje / LANGUAGE EDITING

Terry T. JACKSON

Oblikovanje in tisk / DESIGN AND PRINT

Fotografika, Boštjan Colarič s.p.

Naslovna fotografija / COVER PHOTOGRAPH

Jurij AVSEC

Oblikovanje znaka revije / JOURNAL AND LOGO DESIGN

Andrej PREDIN

Ustanovni urednik / FOUNDING EDITOR

Andrej PREDIN

Spoštovani bralci revije Journal of energy technology (JET)

V Soncu potekajo termonuklearne reakcije, jedrska energija se pretvarja v kalorično in se razsipa v vesolje. Glavni mehanizem prenosa toplote iz Sonca je toplotno sevanje. Le majhen, neznaten del sevanja oz. toplotne energije, ki preide do površja Zemlje, predstavlja izjemen energetski potencial, katerega bi bilo potrebno v prihodnjih desetletjih v večji meri izkoristiti tudi v Sloveniji. V prejšnjih številkah revije sem v uvodniku že pisal o izkoriščanju sončne energije za pretvorbo v električno energijo ali za proizvodnjo vodika. Zelo zanimivo in energetsko izjemno učinkovito je izkoriščanje sončne energije za proizvodnjo toplotne energije. V ta namen obstajajo različni sistemi, kot so na primer ploščni kolektorji, vakuumski kolektorji in toplozračni kolektorji. V tej številki revije pa je predstavljena ideja o fasadnih sončnih panelih, s pomočjo katerih lahko pridobimo toploto za ogrevanje v povezavi s toplotno črpalko. Fasadni paneli, v smislu proizvodnje toplotne energije, še niso razširjeni, ima pa uporaba fasadnih panelov, poleg proizvodnje toplote, še druge dobre lastnosti kot na primer boljšo zvočno in toplotno izolativnost. Prednost vidimo tudi v tem, da bi se solarni fasadni paneli lahko izdelovali v velikih serijah, kar bi pomenilo dodatne zaposlitve in velikomasovno izdelavo aluminjastih izdelkov tudi na tem področju. V primeru uporabe sončnih sistemov za ogrevanje lahko bistveno zmanjšamo tudi emisijo ogljikovega dioksida v ozračje. Vzpodbudno je, da je v razširjanje ideje o izrabi sončne energije vključeno slovensko podjetje Talum d. o. o., prav tako Tehnična Univerza v Gradcu in Univerza v Mariboru.

Jurij AVSEC
odgovorni urednik revije JET

Dear Readers of the Journal of Energy Technology (JET)

In the sun, thermonuclear reactions are taking place, and nuclear energy is being converted into caloric energy and dispersed into space. The main mechanism of heat transfer from the Sun is thermal radiation. Only a small part of the radiation or thermal energy (but still large enough) comes to Earth. The energy of the sun that falls on the Earth's surface represents exceptional potential, which needs to be exploited in the coming decades in a much greater measure, also in Slovenia. In previous issues of JET, I have written about the use of solar energy for conversion to electricity or hydrogen production. It is very interesting and energy efficient to use solar energy for the production of heat energy. For this purpose, there are various systems, such as plate collectors, vacuum collectors, and hot-air collectors. In this issue of the journal, the idea of facade solar panels is presented, through which heat can be obtained for heating in connection with a heat pump system. Facade panels, in terms of heat production, are not yet very common in the world, but the use of façade panels other than heat production has other good properties, such as better sound and thermal insulation. There is the possibility of making solar facade panels on a large scale, which also could mean additional employment and large-scale production of aluminium products in this area. In addition, this can also greatly reduce the use of fossil fuels for heating. I am delighted that the idea of using solar energy also includes Talum d.o.o. and universities such as the Technical University of Graz and the University of Maribor.

Jurij AVSEC
Editor-in-chief of JET

Table of Contents / Kazalo

Journal of Energy Technology

JET Volume 12 (2019) p.p. 11-21
Issue 1, April 2019
Type of article 1.01
www.fe.um.si/en/jet.html

THERMAL ANALYSIS AND APPLICATION OF ROLL BOND SOLAR ABSORBERS FOR HEATING AND COOLING IN RESIDENTIAL BUILDINGS

TOPLOTNA ANALIZA IN UPORABA ROLL BOND SONČNIH ABSORBERJEV ZA OGREVANJE IN HLAJENJE HIŠ

Jurij Avsec[1✉], Daniel Brandl[2], Helmut Schober[3], Urška Novosel[1], Janko Ferčec[4]

Keywords: Roll bond technology, STAF panel, solar technology, heat pump

Abstract

The use of renewable energy sources will have to be increased significantly over the coming decades. The potential of solar energy in Slovenia represents the largest share of renewable energy sources. This article shows the use of roll bond solar absorbers for the heating and cooling of houses. For this purpose, we performed a numerical simulation of solar absorbers and theoretical calculations.

Povzetek

Izrabo obnovljivih virov energije bo potrebno v prihodnjih desetletjih izdatno povečati. Potencial sončne energije predstavlja v Sloveniji največji delež med obnovljivimi viri energije. Predstavljen članek prikazuje uporabo roll bond sončnih absorberjev za ogrevanje in hlajenje hiš. V ta namen smo izvedli numerično simulacijo sončnih absorberjev in teoretične izračune.

✉ Mailing address: Hočevarjev trg 1, 8270 Krško, Slovenia
[1] University of Maribor, Faculty of Energy Technology, Hočevarjev trg 1, SI-8270 Krško, Slovenia
[2] Institute of Thermal Engineering, Graz University of Technology, Inffeldgasse 25b, A-8010 Graz
[3] Institute of Building Construction, Graz University of Technology, Lessingstraße 25III, A-8010 Graz
[4] TALUM d.d. Kidričevo, Tovarniška cesta 10, 2325 Kidričevo

1 INTRODUCTION

The effects of global warming are a crucial issue. The combination of renewable energy sources (RES) and the use of alternative energy technology, such as heat pumps and hydrogen technology, could solve major ecological problems. In Central Europe, the energy demand for heating and cooling in residential buildings is clearly higher than, for example, for the generation of electricity or energy for trucking. In this paper, a new solar thermal absorber has been analysed, which is produced by using the so-called "roll bond" technology. This study contains three core parts: the description of the production process of solar thermal absorbers, an analysis of the thermal behaviour for one selected absorber geometry, and the application in the heating and cooling systems of residential buildings. The focus lies on the determination of the energy efficiency by combining this solar thermal absorber with heat pumps and biomass or geothermal systems in Central Europe.

1.1 Production of solar roll bond absorbers

The roll bond technology enables the production of very flat heat exchanger geometries. It is also possible to use such heat exchangers for solar absorbers in different applications, e.g., a solar collector, photovoltaic thermal hybrid solar collectors, a thermodynamic panel and as an absorber for façade panels. Two different types of roll bond heat exchanger geometries can be used for these applications. The first type is a double-sided inflated plate made of aluminium. The second type is a one-sided inflated plate made of aluminium and an aluminium zirconium alloy combination.

The initial material for the production of roll bond plates is two aluminium strips in coils. This is followed by several production processes, including straightening and brushing before the required fluid pipe system for the absorber is printed on the bottom strip by means of serigraphy. Both strips are preheated up to 300 °C and bonded together under pressure in a heated rolling mill. The bonded strip has to be cooled down before it can be cut into plates with the requested dimensions at the end of the production line. Fig. 1 shows a schematic of the roll-bond process. The plates are put into a furnace for annealing, which is required before the inflation of the fluid pipes. After the annealing process, the fluid pipes are inflated using air at a pressure between 100 to 140 bar. Fig. 2 shows a schematic presentation of annealing the plates and the inflation process. The final steps in the production process are the shearing and brazing of connection tubes on the heat exchanger as well as the leakage tests.

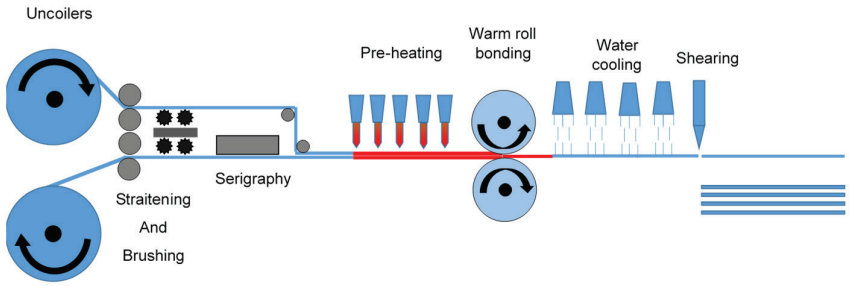

Figure 1: *Schematic of the roll-bond process*

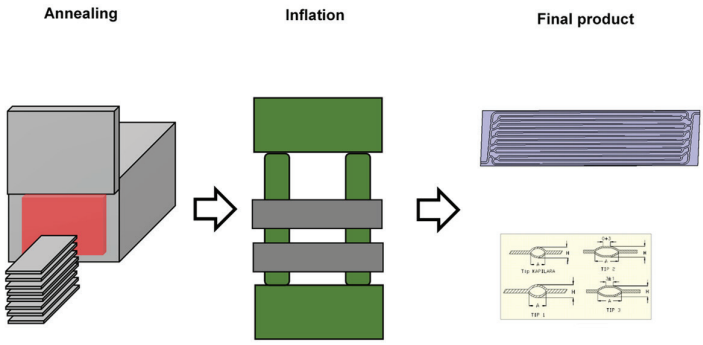

Figure 2: *Schematic of the plates annealing and the inflation process*

2 INTRODUCTION OF THE SOLAR THERMAL ACTIVATED FAÇADE (STAF) PANEL

Conventional sandwich panels offer an inexpensive and simple solution to form thermal envelopes for industrial buildings. They are pre-fabricated façade elements of which millions of square metres are produced and mounted every year. A sandwich panel consists of both an interior and an exterior metal sheet with thermal insulation between them. The central concept of the Interreg project "ABS-Network SIAT 125" *[1]* is the thermal activation of a conventional sandwich panel in which solar radiation is transformed into thermal energy. Therefore, the so-called "solar thermal activated façade (STAF)" panel has integrated fluid pipes at the exterior as well as at the interior metal sheet. Fig. 3 shows the basic design of an STAF panel with its formed aluminium sheets (absorbers) by using roll-bonding technology (as described above).

Depending on the application and seasonal influences, fluid flowing through the pipes enables the thermal use of solar energy (energy harvesting) on the exterior surface. In addition, the fluid can manage the thermal conditioning (heating and cooling) of the rooms on the interior surface (working principle is shown in Fig. 4). The insulator located between the absorber plates represents the thermal building envelope and should keep heat losses as low as possible. Due to this sophisticated modification of sandwich panels, the field of application can be extended to office buildings, public buildings, residential buildings, etc.

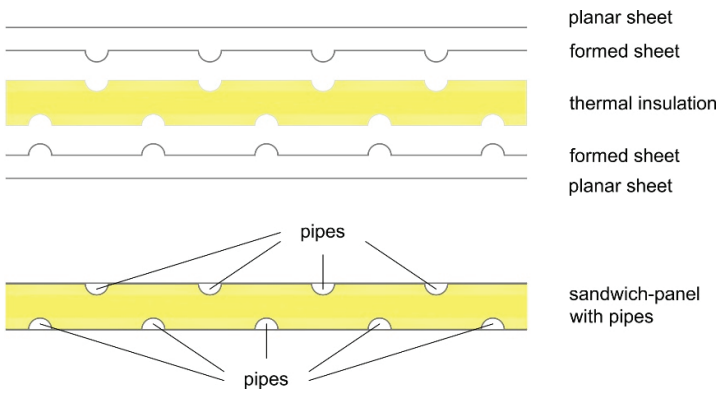

Figure 3: *Illustration of the basic design of the STAF panel*

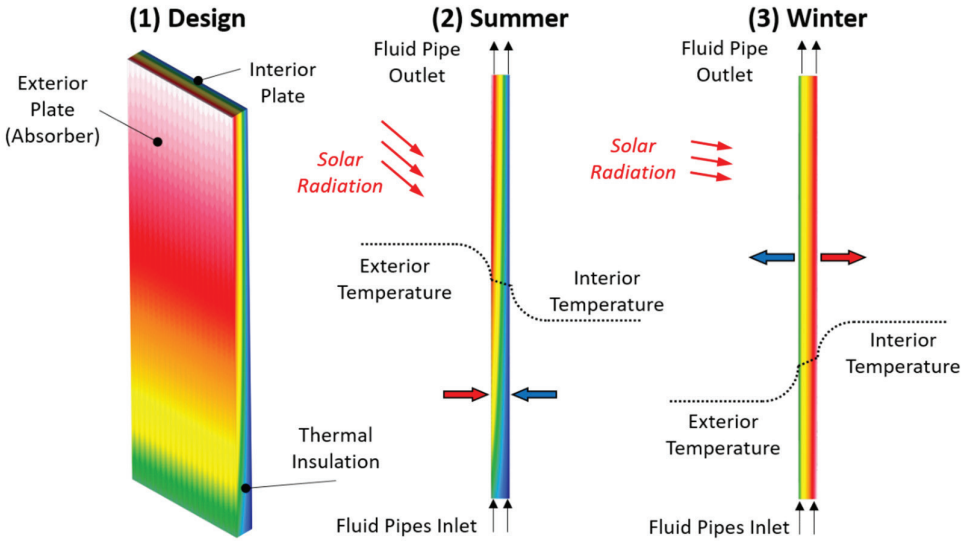

Figure 4: *Illustration of the design and the working principle of the STAF panel*

3 THERMAL ANALYSIS OF THE STAF PANEL (CFD SIMULATION)

With the help of Computational Fluid Dynamics *[2]* (CFD) method, a thermal analysis was performed at the Graz University of Technology to understand the heat transfer mechanism and to improve the efficiency of the absorber plate. This numerical simulation method enables calculating a broad range of different scenarios because geometrical and operative parameters can easily be varied.

In this study, the thermal performance of the exterior plate of a 3.5 × 1.0 m STAF panel was analysed by using a CFD software package from ANSYS Fluent *[3].* The simulation method was

developed and validated in the course of the research project UNAB *[4].* Because the absorber plate dimension is yet limited to 1.75 × 0.5 m by the production plant of Talum d.d., four plates with the same fluid pipe geometry are interconnected to fulfil the required absorber dimensions for the STAF panel (shown in Fig. 5). In the simulation, aluminium is used as absorber material (with a density of 2700 kg/m^3, a specific heat of 896 J/kgK, and a thermal conductivity of 201 W/mK). Furthermore, the simulation considers a thermal insulation with a thickness of 0.15 m, which is made of polyurethane (with a density of 40 kg/m^3, a specific heat of 1400 J/kgK, a thermal conductivity of 0.025 W/mK), and an interior aluminium plate. At the interior surface of the interior plate, an interior room temperature of 20 °C and a heat transfer coefficient of 5 W/m^2K is assumed in the simulation. The sides of the STAF panel are determined to be symmetrical; the bottom and top surface are defined as an adiabatic wall. The panel's exterior absorber plate has two inlets at the bottom (1st absorber) where the fluid is introduced to the pipe network. (the fluid pipe profile used is illustrated in Fig. 5). In this simulation, a mixture of 70 $Vol\%$ water and 30 $Vol\%$ glycol is used to prevent freezing of the fluid at temperatures below 0 °C (with a density of 1035 kg/m^3, a specific heat of 3617 J/kgK and a thermal conductivity of 0.5 W/mK). The fluid flows upwards through the 1st absorber, enters the 2nd absorber, and leaves the absorber at the top of the STAF panel.

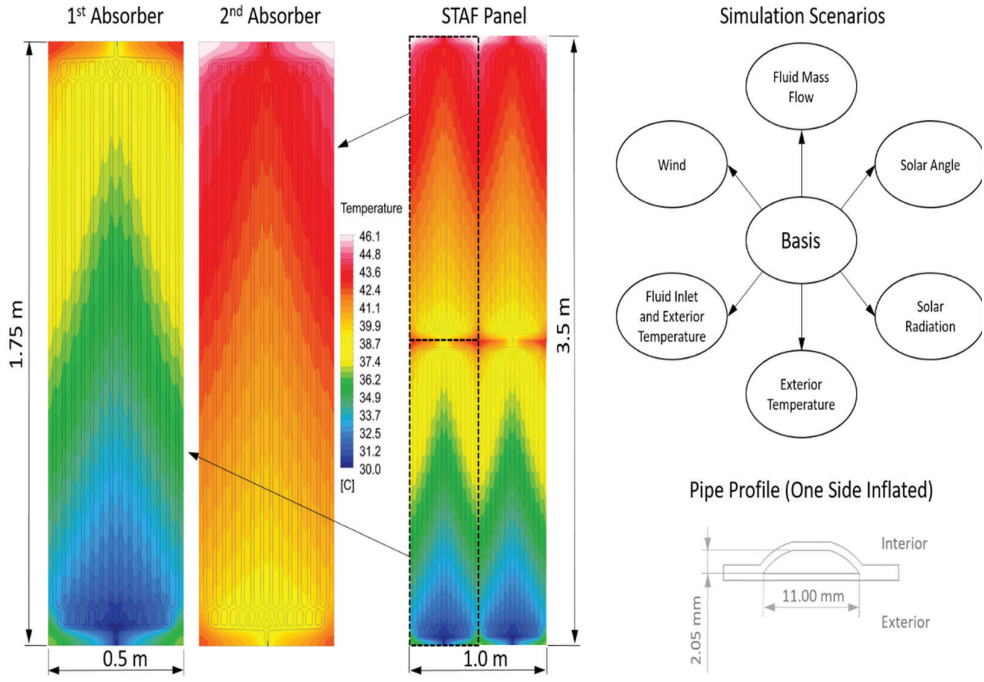

Figure 5: *Temperature contours of the exterior surface of (1) the absorber plates, (2) the STAF panel, (3) simulation scenarios, (4) fluid pipe profile*

The remaining thermal boundary conditions have been varied in a parameter analysis. In the initial scenario (basic scenario), the exterior temperature (T_{ext}) amount of 30 °C and the exterior heat transfer coefficient (representing more or less the influence of the average wind speed over a year in Graz, Austria) is 25 W/m^2K. Furthermore, solar radiation of 1000 W/m^2 and a solar angle of 45° are assumed. The water-glycol mixture is introduced with a volume flow rate ($\dot{V}_F$) of 100 l/h per inlet and at an temperature ($T_{F,in}$) of 30 °C. The varying parameter are illustrated in the schematic of the simulation scenarios in Fig. 5; all scenarios are summarized in Table I. Additionally, the table contains the computed fluid temperature ($T_{F,out}$) at the outlet positions of the absorber's pipework as well as the calculated thermal output ($\dot{Q}_{STAF}$) and efficiency (η_{STAF}) of the whole STAF panel according to the following equations ((3.1) and (3.2)).

$$\dot{Q}_{STAF} = \dot{m}_F \cdot c_{p,F} \cdot \left(T_{F,out} - T_{F,in}\right) \tag{3.1}$$

$$\eta_{STAF} = \frac{I_{Sol} \cdot A_{STAF}}{\dot{Q}_{STAF}} \tag{3.2}$$

In the basic scenario, a fluid outlet temperature of 43.3 °C was achieved, resulting in a thermal output of 1379.7 W and an efficiency of 0.394. If the mass flow increased up to 200 l/h, the fluid outlet temperature was 4.9 K lower. Although the fluid outlet temperature was lower, the efficiency was significantly higher because the heat losses to the environment have decreased. At a mass flow of 50 l/h, the fluid outlet temperature is 4.9 °C higher than in the basis scenario, resulting in a lower efficiency. In the CFD simulation, the simultaneous reduction of the exterior and the fluid inlet temperatures leads to a lower fluid outlet temperature while the efficiency was slightly increased. Compared to the basis scenario, the fluid outlet temperature was 6.6 °C lower when the solar radiation was reduced from 1000 to 500 W/m^2; the efficiency was almost equal. When the fluid inlet temperature was reduced while the exterior temperature was constant at 30 °C, the absorber is more efficient than reducing both the inlet and exterior temperatures. In this case, the exterior temperature was amplifying the heating effect. Furthermore, the heat transfer effect of the absorber is strongly influenced by the wind. For a heat transfer coefficient of 5 W/mK^2, which represents less wind, the fluid outlet temperature was 4.9 K higher than in the basic scenario. For a heat transfer coefficient of 100 W/m^2K, the fluid outlet temperature was 7.4 K lower than in the basic scenario. Finally, the influence of the solar angle was analysed. For a flat solar angle of 20°, the fluid outlet temperature was 4.3 K higher, while it was 5.3 K lower at a steep solar angle of 65°.

Table 1: *Results from CFD simulation scenarios*

Simulation scenario	$\dot{V}_F$	T_{ext}	$T_{F,in}$	$T_{F,out}$	$\dot{Q}_{STAF}$	η_{STAF}
	$[l/h]$	$[°C]$	$[°C]$	$[°C]$	$[W]$	$[-]$
Basic scenario	100	30	30	43.3	1379.7	0.394
Volume flow rate of 200 l/h per inlet	200	30	30	38.4	1742.6	0.498
Volume flow rate of 50 l/h per inlet	50	30	30	48.1	943.0	0.269
Exterior and fluid inlet temperature of 20 °C	100	20	20	33.4	1393.3	0.398
Exterior and fluid inlet temperature of 10 °C	100	10	10	23.5	1407.8	0.402
Exterior and fluid inlet temperature of 0 °C	100	0	0	13.7	1421.3	0.406
Exterior and fluid inlet temperature of -10 °C	100	-10	-10	3.8	1436.9	0.411
Solar radiation of 500 W/m²	100	30	30	36.7	691.4	0.395
Fluid inlet temperature of 20 °C	100	30	20	39.5	2027.5	0.579
Fluid inlet temperature of 10 °C	100	30	10	35.7	2670.1	0.763
Fluid inlet temperature of 0 °C	100	30	0	31.8	3309.5	0.946
Fluid inlet temperature of -10 °C	100	30	-10	28.0	3945.8	1.127
Exterior heat transfer coefficient of 5 W/m²K	100	30	30	48.2	1892.3	0.541
Exterior heat transfer coefficient of 100 W/m²K	100	30	30	35.9	615.5	0.176
Solar angle of 65°	100	30	30	37.9	824.5	0.236
Solar angle of 20°	100	30	30	47.6	1829.9	0.523

4 APPLICATION OF THE STAF PANEL (CASE STUDY)

The purpose of installing STAF panels on buildings is to save as much as possible in the consumption of already used primary energy sources for space and domestic hot water heating and thus contribute to lower greenhouse gas emissions. Buildings with integrated STAF panels are approaching the status of low-carbon (energy-efficient) buildings, which affects the outcome in obtaining an energy certificate. With the installation of STAF panels, we are approaching the standards that reflect EU objectives, which are always higher regarding the policy of obtaining permits for new buildings. By installing a modified version of STAF panels for the thermal improvement of an existing building, it is necessary to emphasize the construction work is not significant, the architecture remains almost the same, which means that substantial construction work in the renovation is not required, since the panels are installed on the outside of the wall (façade), following which the thermal insulation of the building is improved. It is also essential to use a renewable energy source (solar energy) for heating, which is fairly energy efficient for use in Central Europe and elsewhere.

STAF panels, which can also be installed on the outer wall of a building have some decisive advantages. The use of solar radiation, of course, also depends on the installation of solar panels according to the cardinal orientation and the slope of the panels (different values for different areas in the world). In Central Europe, if the panel is installed, for example, on the southern vertical wall of the building, about 30% of solar radiation is lost compared to the optimal slope. Solar collectors are usually installed on the roofs of building, as the greatest amount of sun rays reaches them due to the slope, and due to the reduced influence of surrounding buildings, that could cast a shadow on the collectors. Precisely because it is a “too favourable” position for the installation of panels, in summer, problems with overheating of panels may occur and, consequently, lower efficiency and damage to panel components *[4].*

STAF panels can be used as additional heat generators to the existing heating system with the production of heat for space heating and domestic water. For example, imagine a residential house built in the vicinity of the municipality of Krško, Slovenia, with the maximum heating power to heat this building (12 kW). Depending on the annual load of the heating plant, the necessary energy for the heating of the residential building including sanitary water preparation is 36,580 kWh per year *[5].* For the energy analysis of the application of solar panels for heating of residential buildings, the STAF panels were combined with a heat pump system (Fig. 6). For the determination of the solar radiation, the number of effective hours for the Krško region, Slovenia were calculated. According to the solar calculator from the solar electricity handbook *[6]*, the effective number of solar hours is 1,224. The principle idea behind the STAF panels is to cover the majority the heat demand in the summer and the highest share in the winter. Table 2 shows the amount of energy that is obtained from the STAF panels and with a heat pump if the STAF panels cover 30%, 50%, or 80% of the energy demand for heating. Figure 7 shows the price for heating and the minimal required number of installed STAF panels dependant on solar coverage with STAF panels.

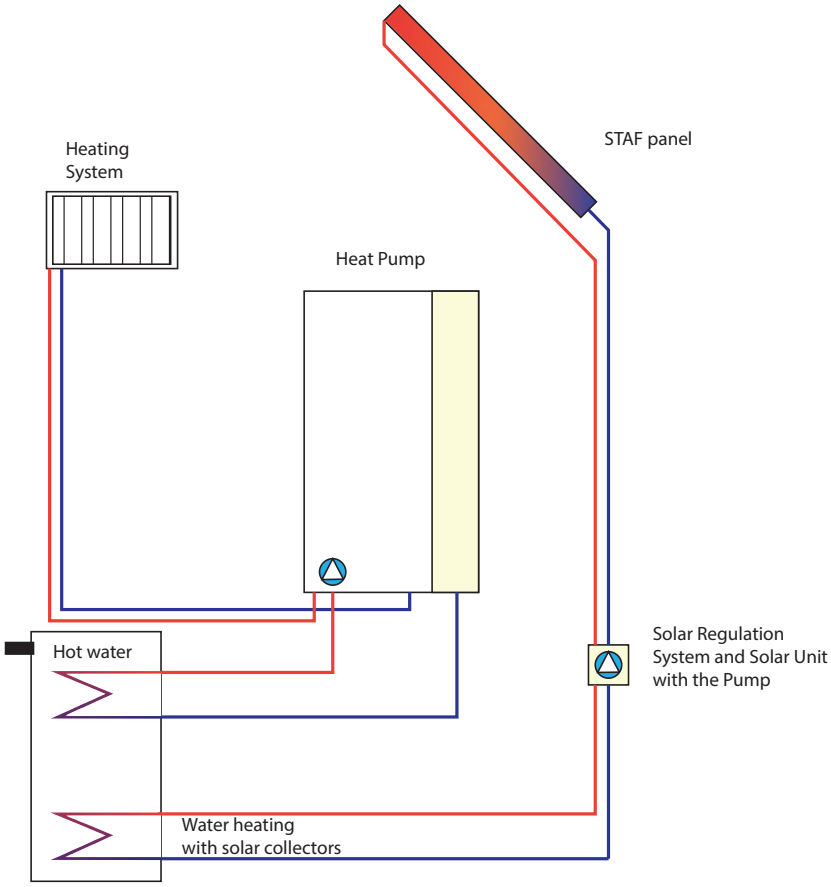

Figure 6: *Hydraulic schematic of a heat pump cycle for heating of a family house with integrated STAF panel*

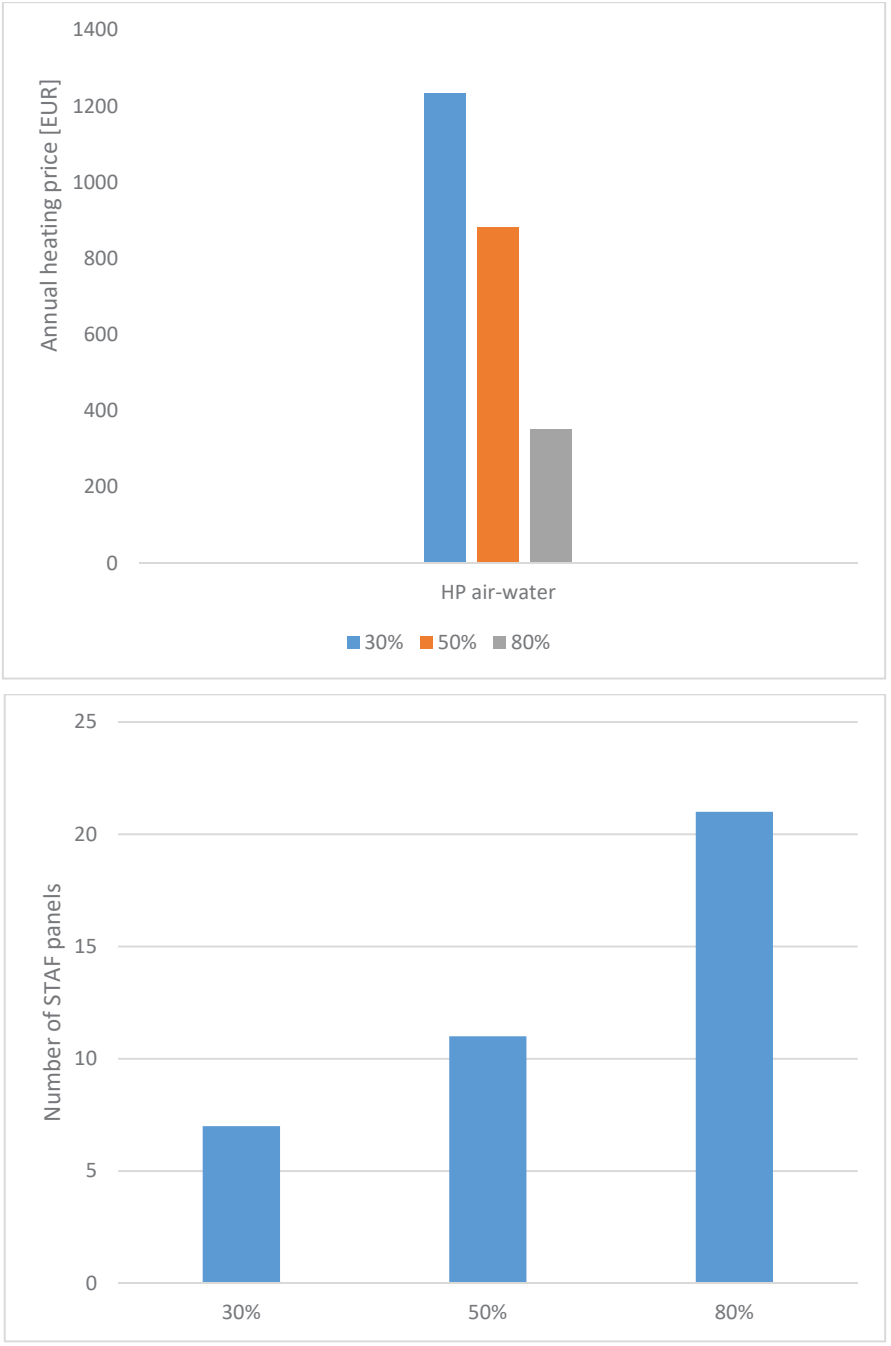

Figure 7: *Heating price depending on the energy demand of a family house and the minimal number of required STAF panels*

Table 2: *Use of solar energy (STAF panels) for heating of a family house*

:	30% use of solar energy	50% use of solar energy	80% use of solar energy
STAF panels	10974 kWh	18290 kWh	29264 kWh
Heat pump (HP)	25606 kWh	18290 kWh	7316 kWh

5 CONCLUSION AND OUTLOOK

In this article, we have shown the possible application of STAF panels with heat pump technology. The results show that an application of STAF panels is very interesting from thermodynamic, ecologic, as well as economic perspectives.

Multiple CFD simulations were performed to analyse the thermal behaviour and determine the thermal output of STAF panels. In the simulations, a water-glycol mixture was heated inside an STAF panel with the dimensions of 3.5 × 1.0 × 0.15 m up to 48.2 °C. The maximal thermal output was approximately 3.9 kW. The exterior temperature and the wind have a powerful impact on the thermal behaviour and output. When the ambient temperature is higher than the average surface temperature of the exterior absorber plate, the fluid is additionally heated. Unfortunately, the absorber's heat loss increases as the ambient temperature decreases. The heat loss at low ambient temperatures can be reduced by installing a glass cover for the absorber.

In the course of the project "ABS-Network SIAT 125" *[1]*, further thermal and structural analysis of the STAF panel will be performed to optimize the whole construction and improve the thermal output. Additionally, outdoor tests will be performed at the Graz University of Technology to compare the thermal behaviour of the most promising STAF panel absorber geometries under real climate conditions.

References

[1] Interreg-project "ABS-Network SIAT 125" (http://abs-network.eu/en)

[2] ANSYS Fluent 18.2. Userguide/Theoryguide

[3] Fluid Dynamics software "ANSYS Fluent 18.2.0", ANSYS Inc., Southpointe 275 Technology Drive Canonsburg, PA 15317, http://www.ansys.com, Release 18.2 (2018)

[4] Uporaba STAF sončnih panelov za ogrevanje – Študijska naloga, fazno poročilo, Fakulteta za energetiko Univerze v Mariboru, May 2018

[5] **A. Bratkovic, R. Irgl:** *Daljinski sistemi ogrevanja na lesno biomaso*, Enecon, 2006

[6] http://solarelectricityhandbook.com/solar-irradiance.html

Journal of Energy Technology

JET Volume 12 (2019) p.p. 23-31
Issue 1, April 2019
Type of article 1.01
www.fe.um.si/en/jet.html

INTEGRATION OF TALUM'S ROLL-BOND HEAT EXCHANGER FOR DIFFERENT APPLICATIONS

INTEGRACIJA TALUMOVIH TOPLOTNIH PRENOSNIKOV, IZDELANIH PO POSTOPKU PLATINIRANEGA VALJANJA ZA RAZLIČNE APLIKACIJE

Janko Ferčec[1✉], Rajko Habjanič[1]

Keywords: Talum, Roll-bond, Heat exchanger, Evaporator, Absorber

Abstract

This article presents the integration of heat exchangers made using the roll-bond technology of Talum d.d., Kidričevo, Slovenia, to applications in refrigeration and heating technology. Talum has more than 30 years of tradition in the production of evaporators for cooling technology and heat exchangers for various purposes, such as absorbers and condensers. The heat exchangers produced in Talum are made of aluminium or aluminium alloys and are categorized as flat heat exchangers. Aluminium and aluminium alloys can be completely recycled after they reach the final phase of their life cycle, which is an essential feature in terms of sustainable construction. The roll-bond technology enables the manufacture of heat exchangers with a complex geometry of channels, which enables them to be used for various applications. Enabled through roll-bond technology, all of these features give the roll-bond heat exchanger a very useful and functional value. In this article, we focused only on some implemented and potential applications of heat exchangers made with using the roll-bond technology.

✉ Corresponding author: Janko Ferčec, Address, Tel.: +386 2 7995 589, E-mail address: janko.fercec@talum.si

[1] TALUM d.d. Kidričevo, Tovarniška cesta 10, 2325 Kidričevo

Povzetek

Članek predstavlja integracijo toplotnih prenosnikov izdelanih s tehnologijo platiniranega valjanja v podjetju Talum d.d. Kidričevo v nekatere aplikacije na področju hladilne in toplotne tehnike. Podjetje Talum ima več kot 30-letno tradicijo izdelave uparjalnikov za hladilno tehniko in toplotnih prenosnikov za različne namene kot so absorberji in kondenzatorji. Toplotni prenosniki, ki se proizvajajo v Talumu so izdelani iz aluminija oziroma aluminijeve zlitine in spadajo med ploščate toplotne prenosnike. Aluminij in aluminijeve zlitine je mogoče popolnoma reciklirati po izteku življenjskega cikla izdelka, kar je z vidika trajnostne gradnje pomembna lastnost. Tehnologija platiniranega valjanja omogoča izdelavo toplotnih prenosnikov s kompleksno geometrijo kanalov, kar omogoča izdelavo toplotnih prenosnikov za različne aplikacije. Vse te lastnosti, ki jih omogoča tehnologija platiniranega valjanja dajejo toplotnim prenosnikom veliko uporabno in funkcionalno vrednost. V članku smo se osredotočili le na nekatere implementirane in potencialne aplikacije toplotnih prenosnikov izdelanih s tehnologijo platiniranega valjanja.

1 INTRODUCTION

The company Talum, d.d. from Kidričevo, Slovenia was established in 1954 when the first aluminium was produced. Since then, Talum has been producing primary aluminium and different semi-products and final products from aluminium and aluminium alloys using different production technologies. Talum offers to its customers support in the development of processes, as well as support in the development of products for projects, *[1].*

In 1981, Talum started with the production of wide aluminium strips, which are a semi-finished product for manufacturing evaporators. Regular production of evaporators started in 1982. Since then, Talum has been producing evaporators for refrigerators and other heat exchangers for different applications of solar and heating techniques, *[1].*

The production of roll-bond plates for heat exchangers and evaporators is a continuous process consisting of several phases. The starting material for roll-bond heat exchangers is two sheets in coils, which are bonded together in a rolling mill under elevated temperature and high deformation. The next phase is recrystallization annealing in a furnace to reduce the strength of the material, which is necessary for the next phase. This phase is followed by the phase of the inflation of imprinted channels on a hydraulic press machine. The last phase of production of a roll-bond heat exchanger is cutting or stamping the plates in their final dimensions, *[2,3].*

Roll-bond technology or roll-bond plates are widely used as evaporators for refrigeration. For the past decade, it has also been popular in other applications, such as cooling plates for photovoltaic thermal (PVT) panels. In addition, it can be used in integrating roll-bond plates into other systems, such as battery cooling plates in battery modules, waste heat absorbers, and condensers, *[4].*

This paper focuses on Talum's research and development of roll-bond heat exchangers and introduces some examples of integration. The paper provides basic information on Talum's roll-bond technology and potential uses of roll-bond plates since the roll-bond technology shows potential in buildings for the heating and cooling industries.

2 TYPES OF ROLL-BOND PLATE HEAT EXCHANGER

Talum produces two different types of roll-bond heat exchanger according to the shape of channel. The first type is a double side (DS) inflated roll-bond plate (Figure 1) and the second is roll-bond plate inflated on one side (one side flat (OSF)) (Figure 2). The dimension of the cross section channel is standardized. Modification of the cross-section is limited by the formabilit properties of the material used for the heat exchanger.

LEGEND:

A = width of the channel or capillary

H = height of the channel or capillary

O^{+3} = width allowed on flat part of the channel

3$^{\pm 1}$ = width allowed on flat part of the channel

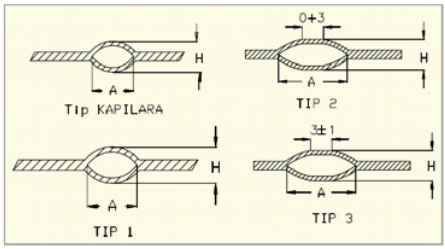

Figure 1: *Double side inflated roll-bond plate, [1]*

LEGEND:

D = thickness of the panel

H = height of channel, height of capillary

A = width of the channels, capillary

O^{+4} = width allowed on flat part of the channel

3$^{\pm 2}$ = width allowed on flat part of the channel

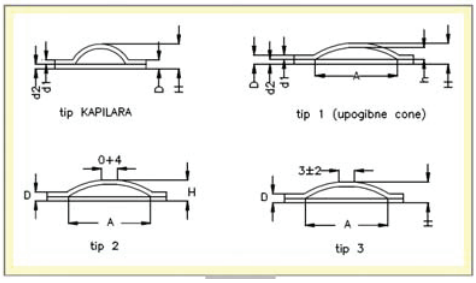

Figure 2: *One side inflated roll-bond plate, [1]*

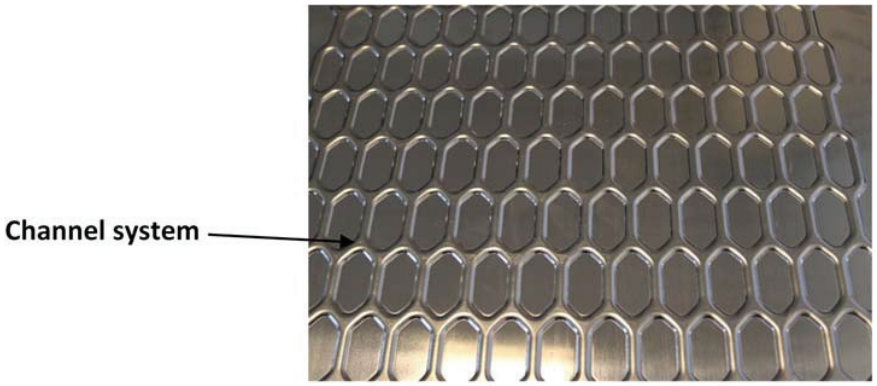

Figure 3: *Example of a channel system in a roll-bond heat exchanger plate*

Talum can produce a channel system for a heat exchanger in accordance with customer demand or can help customers design and produce different models of roll-bond heat exchanger. With the roll bond technology, it is feasible to produce a complex channel system like the one shown in Figure 3. The channel system has limited formability properties.

3 ROLL-BOND EVAPORATORS FOR REFRIGERATION

Roll-bond evaporators (Figure 4) were widely used in household appliances (e.g., coolers and refrigerators) until 2008, when, following the financial crisis, the existence of higher pressure on prices resulted in reduced demand for Roll bond evaporators due to the cheaper substitutes of tube on wire (TOW), tube on sheet (TOS), tube on foil (TOF) as well as dynamic cooling systems like ("no frost") fin on tube. All these substitutes are cheaper than roll-bond, but they cannot attain its heat transfer efficiency. The need for roll-bond has grown recently because energy efficiency demands (regulations) are increasing. The most efficient coolers are almost by default equipped with roll-bond evaporators.

The use of DS or OSF evaporators is defined by the purpose of use. DS evaporators are used when mounted inside the containment of the appliance. OSF is commonly glued behind the inner walls of the appliance and then foamed with thermal insulating foam. In specific cases in which a roll-bond evaporator is made as one side extra flat (OSEF); then the properly painted flat surface can also be used as a back wall inside the cooling cabinet.

The channel design enables equal (or desired) heat transfer flow; it must ensure that all refrigerant evaporates and also enables-low-pressure drop throughout the plate. The channels must be designed so that they are not deformed, while the evaporator plate is bent to a certain radius. The plate thickness and channel width are determined by the operating pressure.

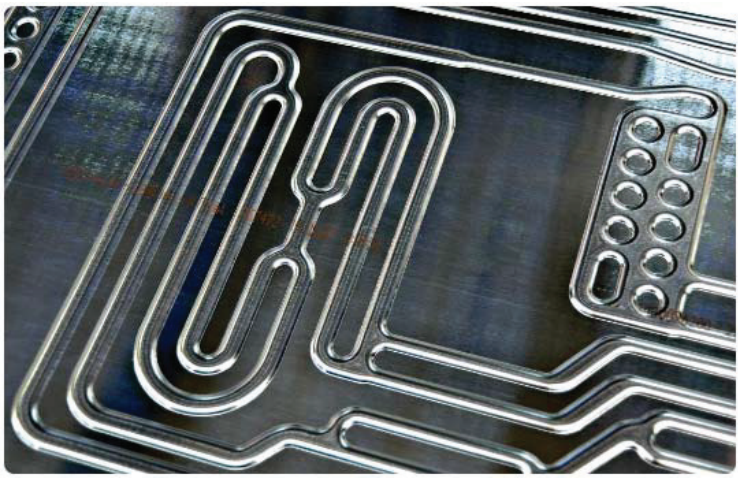

Figure 4: *Roll-bond plate for evaporator in refrigeration*

4 ROLL-BOND HEAT EXCHANGER FOR HEAT TECHNIQUE

In heat techniques, roll-bond plates are used as absorbers in different installations. Roll-bond plates are used as thermal absorbers and can be used as highly-efficient absorbers, when coated properly, in solar thermal collectors. Talum also develops and manufactures cooling plates for photovoltaic (PV) thermal (PVT) panels, as shown in Figure 5. Cooling of the PV panel can increase the efficiency of the PV panel. The thermal energy from the cooling of PV can be used for the heating of pool, domestic hot water, or support for building heating.

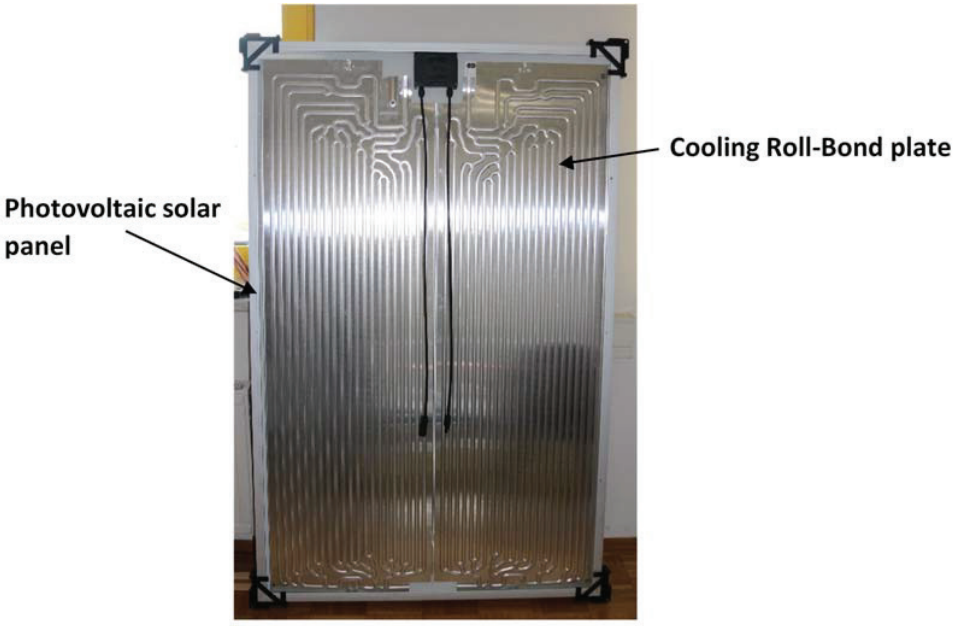

Figure 5: *Cooling roll-bond plate on the back side of Photovoltaic panel*

In Talum, the analysis and measurements of the manufactured roll-bond heat exchanger are performed. The purpose of measurements and analysis is to obtain feedback information to improve the efficiency of the product. For the analysis of the PVT with roll-bond cooling plate, a thermovision (IR) camera is used to see the temperature distribution and differences. In one analysis, thermovision analysis on the PV without the heat exchanger or cooling plate was performed. It was determined that on the back side of the panel on a normal sunny day, a PV panel reaches a temperature of 70°C, which has a negative impact on the effectiveness of the PV panel (Figure 6). The same thermovision analysis was performed on PV, but with an added roll-bond cooling plate. Figure 7 shows the thermovison analysis with a cooling plate, where a medium with the temperature around 20 to 25°C was used. With the integrated roll-bond plate, a reduction of the average temperature to approximately 30° on the PV panel was achieved. Such analysis and measurements facilitate the development and integration of our products into different applications. Based on these results, which are rapidly obtained, we decide whether to conduct more complex and precise research, such as measurements of the efficiency on the whole integrated system.

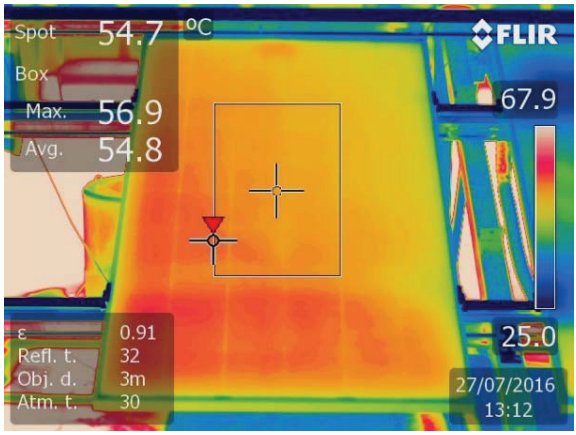

Figure 6: *Thermo-vision pictures of the front side of the photovoltaic panel*

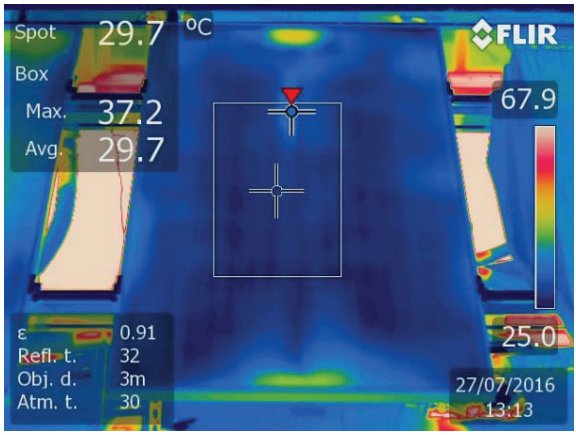

Figure 7: *Thermo-vision picture of the front side of the photovoltaic panel with the roll-bond cooling plate*

Roll-bond plates are also used as thermodynamic panels for heat pumps or as condensers in domestic hot water heat pumps (DHWHP). The heat transfer media in such roll plates is refrigeration gas for thermodynamic panels and DHWHP condensers, while for solar thermal absorbers, a mixture of water and glycol is used.

On various websites, it is possible to find some activities on implementation and integration of roll-bond plates to different systems in which a roll-bond heat exchanger is used as absorber, condenser and convector. Most systems include a heat pump, which increases the temperature since a low temperature is obtained from roll-bond absorbers, which is not directly applicable. From this reason, an additional system that increases the temperature of the medium to a useful level is needed.

5 COOPERATION ON INTERNATIONAL PROJECT

For the development of applications for roll-bond heat exchangers, Talum participates in the Interreg project SI-AT 125 "ABS-Network", *[5]*, which is a cross-border program between Slovenia and Austria. The program is financially supported by the European Regional Development Fund allocated by the European Union. The project aims at developing a prototype of a Solar Thermal-Activated Façade (STAF) panel. The lead partner of the project is Technical University (TU) in Graz (Austria). Talum is a project partner of the ABS-network project. The Faculty of Energy Technology at the University of Maribor (Slovenia) also participates in the project in the analysis on the usability of STAF panel.

The main idea of the ABS-network project is to meet the functional requirements of a façade. Buildings have a façade area (south side) on which the sun shines similarly as on the roof of the building. The idea of the project is to transfer the energy generated by the sun from the outer surface of the panel to the inner side, using a heat exchanger. Figure 8 shows the basic elements of STAF panel, *[6]*, including a two roll-bond heat exchanger (on the outside surface is a so-called absorber plate). Together with the partners on the project, we perform activities related to the analysis of the potential heat or cooling system using the energy from the panel.

The role of Talum in the project is the manufacture of the absorber and heat exchanger for the STAF panel. The absorber and the heat exchanger were designed and developed together with researchers from TU Graz. Many years of experience facilitate work in the development phase of the heat exchanger. One side-inflated channel system was used for the STAF panel. The channel system is integrated on the side with insulation. From the outside, only the aluminium plate can be seen. For that reason, the panel will look like a normal panel on a building, but it also has functional properties.

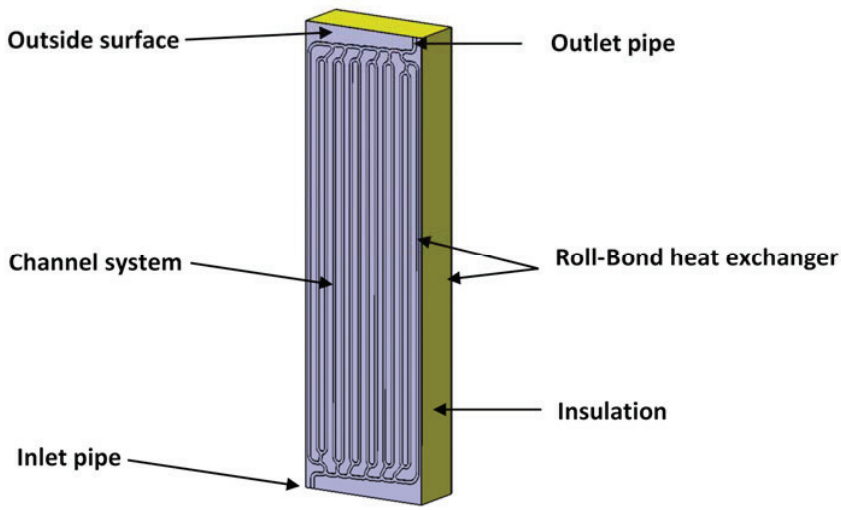

Figure 8: *Roll-bond plate for heat exchanger in solar thermal activated façade panel*

6 FUTURE OF ROLL-BOND PLATE FOR HEAT EXCHANGER

The future of the roll-bond production remains open. Increased demand for low-energy household appliances continues in developing and growing countries where there is still a lack of electric energy. The lowest energy consumption is achieved with roll-bond evaporators. Furthermore, electrical household appliances have a major impact on electrical grid load. As already mentioned in this article, roll-bond technology is finding its way in other industries. In parallel to it, other competitive technologies are developing heat exchangers and different solutions. Producers, led by consumers, are forced to reduce costs, which leads to the use of components that are just at the limit of acceptability.

Mainly due to regulations and overall understanding and awareness of the urgency to minimize energy consumption as well as the environment impact, producers will be forced to use not the cheapest but the best techniques. This should put the roll-bond products in a stable position in the future and give them a chance to develop and to overcome certain deficiencies.

References

[1] Talum d.d. Kidričevo, http://www.talum.si/

[2] **Hiwase R. E., Agrawa J. F:** Research methodology followed for optimization of production system for roll bond evaporator of domestic refrigerator, International journal of pure and applied research in engineering and technology, Vol. 4 No.3, p. 116-130, 2015

[3] **Ravi P.S., Krishnaiah A., Akella S., Azizuddin Md.:** Evaluation Of Inside Heat Transfer Coefficient of Roll Bond Evaporator for Room Air Conditioner, Evaluation Of Inside Heat Transfer Coefficient of Roll Bond Evaporator for Room Air Conditioner, Vol. 4, Issue 5, 2015

[4] **Wu J., Zhang X., Shen J, Wu Y., Connelly K., Yang T., Tang L., Xiao M., Wei Y., Jiang K., Chen C., Xu P., Wang H.,** A review of thermal absorbers and their integration methods for the combined solar photovoltaic/thermal (PV/T) modules, Renewable and Sustainable Energy Reviews. Vol.75, p. 839-854,2017

[5] Interreg Project SI-AT 125 ''ABS-Network'', http://abs-network.eu/en

[6] **D. Brandl, H. Schober, Ch. Hochenauer**: Analysis of Heating Effects and Deformations for a STAF Panel with a Coupled CFD and FEM Simulation Method, Journal of Façade Design and Engineering, Vol. 6, No. 3, p. 116−131, 2018

Journal of Energy Technology

JET Volume 12 (2019) p.p. 31-39
Issue 1, April 2019
Type of article 1.01
www.fe.um.si/en/jet.html

ANALYSIS OF PIPELINE VIBRATION

ANALIZA VIBRACIJ V CEVOVODIH

Jurij Avsec[1✉], Urška Novosel[1]

Keywords: pipeline vibration, pipeline fluid flow, continuous vibration

Abstract

Vibrations occur in almost all energy systems. This article presents an analysis of vibrations in pipelines under the influence of fluxes of displaced persons with a pressure difference or with the help of electromagnetic forces. For this purpose, we analysed pipelines of different diameters and the flow of crude oil within the pipelines.

Povzetek

Vibracije se pojavljajo v skoraj vseh energetskih sistemih. V članku je prikazana analiza vibracij v cevovodih pod vplivom tokov gnanih s tlačno razliko ali s pomočjo elektromagnetnih sil. V ta namen smo analizirali cevovode različnih premerov. V cevovodih smo obravnavali tok surove nafte.

1 INTRODUCTION

Energy devices are affected by many mechanical influences, including mechanical fluctuations. The analysis (analytical and experimental) of mechanical oscillations of energy devices is in many cases of paramount importance. In the present article, we have studied pipeline vibrations for a simply supported pipeline with the help of continuous vibration theory, [1-4]. Fluid flow in pipelines and channels is driven due to the presence of the electric field, magnetic field, or pressure-driven flow, and some other effects, [1] (Fig. 1). Electrohydrodynamics (EHD), known as electrokinetics, is the theory of the fluid dynamics of electrically charged fluids. It is the study of the motions of ionized

✉ Corresponding author: Corresponding author: Prof. Jurij Avsec, Ph. D., Tel.: +386-7-620-2217, Fax: +386-2-620-2222, Mailing address: Hočevarjev trg 1, 8270 Krško, Slovenia
E-mail address: jurij.avsec@um.si, urska.novosel@um.si

[1] University of Maribor, Faculty of Energy Technology, Laboratory for Thermomechanics, Applied Thermal Energy Technologies and Nanotechnologies, Hočevarjev trg 1, SI-8270 Krško, Slovenia

particles or molecules and their interactions with electric fields and the surrounding fluid. The fundamental concept for magnetohydrodynamics (MHD) is that magnetic fields can induce currents in a moving conductive fluid, which in turn creates forces on the fluid and changes the magnetic field itself. This paper develops a formulation of crude oil motion, in macro channels and mini-channels with pipeline fluid flow. A mathematical model is developed for channels with rectangular and circular cross-sections.

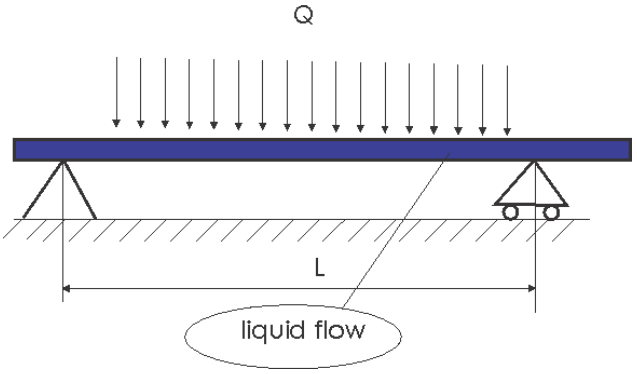

***Figure 1**: Thermal influence on pipeline vibration and fluid flow*

2 FLUID FLOW DUE TO PRESSURE AND MAGNETIC EFFECTS

Consider electromagnetic flow in rectangular and circular channels (Fig. 2). The charged surface of a channel wall may attract ions of the opposite charge in the surrounding fluid. The general form of the momentum equation for electrohydrodynamic flow is:

$$0 = -\frac{dp}{dx} + \mu\frac{d^2u}{dz^2} + i_y B_z,$$

$$\rho\frac{\partial\vec{v}}{\partial t} + \rho\vec{v}\nabla\vec{v} = -\nabla p + \nabla(\mu\nabla\vec{v}) + \vec{\imath}x\overrightarrow{B}, \quad (2.\ 1)$$

where the last term presents the electromagnetic force, and *i* and *B* refer to the current density and magnetic field strength, respectively. For steady-state flow in a channel at small Reynolds numbers, the transient and inertia terms can be neglected, so Eq. (2. 1) is simplified in the next equation:

$$0 = -\nabla p + \nabla(\mu\nabla\vec{v}) + +\vec{\imath}x\overrightarrow{B}. \quad (2.\ 2)$$

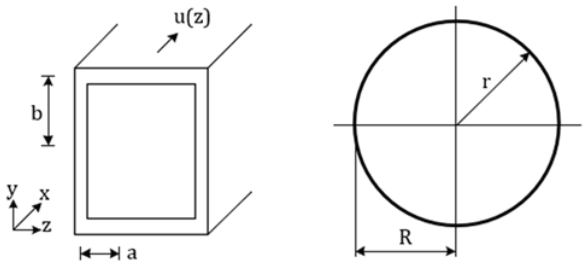

Figure 2: *Rectangular and circular micro channels*

Laminar flow

During electrokinetic flow in channels, the charged surface of a channel wall may attract ions of the opposite charge in the surrounding fluid. Assuming the fluid velocity, magnetic field and current density are orthogonal, the reduced momentum equation becomes:

$$0 = -\frac{dp}{dx} + \mu \frac{d^2u}{dz^2} + i_y B_z. \tag{2. 3}$$

The terms represent pressure, viscous and electromagnetic forces in the liquid. Using Ohm's Law to express the current density in terms of fluid velocity:

$$\mu \frac{d^2u}{dz^2} + \sigma_e B_z^2 u = \frac{dp}{dx}, \tag{2. 4}$$

where: σ_e and B_z refer to the electrical conductivity and magnetic field strength. For fully developed flow in a channel, the pressure gradient becomes constant and independent of the magnetic field strength. In terms of the Hartman number, M_H ($M_H = aB_z\sqrt{\sigma_e / \eta}$),

$$\mu \frac{d^2u}{dz^2} - \left(\frac{M_H{}^2 \eta}{a^2} \right) u = \frac{dp}{dx}. \tag{2. 5}$$

Applying the no-slip boundary conditions at z=0 and z=-2a, the analytical solution of Eq. (2. 5) becomes:

$$u = -\frac{a^2\left(\frac{dp}{dx}\right)}{M_H{}^2\mu} + \frac{a^2\left(\frac{dp}{dx}\right)}{\left(1+2e^{2M_H}\right)M_H{}^2\mu}e^{\frac{zM_H}{a}} + \frac{a^2\left(\frac{dp}{dx}\right)e^{2M_H}}{\left(1+2e^{2M_H}\right)M_H{}^2\mu}e^{\frac{-zM_H}{a}}.$$

The mean velocity within the channel becomes:

$$u_b = \frac{1}{2a}\int_0^{2a} u(z)dz \qquad u_b = \frac{a^2\left(\frac{dp}{dx}\right)\left(-M_H + Tanh\left(M_H\right)\right)}{M_H{}^3\mu} \tag{2. 6}$$

Non-dimensionlizing this result ($z^*=z/a$, $u^*=u/u_b$), we obtain the following equation:

$$u^* = \frac{M_H\left(-1+\frac{1}{\left(1+2e^{2M_H}\right)}e^{z^*M_H} + \frac{e^{2M_H}}{\left(1+2e^{2M_H}\right)}e^{-z^*M_H}\right)}{\left(-M_H + Tanh\left(M_H\right)\right)}. \tag{2. 7}$$

Without electromagnetic effects, equations (5-6) transform into the following expressions:

$$u(z) = \frac{\left(\frac{dp}{dx}\right)}{2\mu}\left(-2az+z^2\right),\ u_b = \frac{1}{2a}\int_{-a}^{a} u(z)dz = \frac{a^2\left(\frac{dp}{dx}\right)}{3\mu},\ u^* = \frac{3}{2}\left(2-z^*\right)z^*, \tag{2. 8}$$

For the circular channel without electromagnetic forces, the governing equation is:

$$\frac{dp}{dx} = \mu\left(\frac{\partial^2 u}{\partial r^2} + \frac{1}{r}\frac{\partial u}{\partial r}\right) \tag{2. 9}$$

Solving the differential equation subject to boundary conditions,

$$u = \frac{\left(\frac{dp}{dx}\right)}{4\mu}\left(r^2-R^2\right),\ u_b = \frac{1}{\pi R^2}\int_0^R u2\pi r dr = -\frac{\left(\frac{dp}{dx}\right)R^2}{8\mu}$$

$$u^* = 2-2r^{*2}. \tag{2. 10}$$

If we wish to calculate the velocity profile for MHD flow in a circular channel, we have to solve the next differential equation:

$$\frac{dp}{dx} = \mu\left(\frac{\partial^2 u}{\partial r^2} + \frac{1}{r}\frac{\partial u}{\partial r}\right) - \mu\frac{{M_H}^2}{R^2}u. \tag{2. 11}$$

The analytical solution of equation (2. 12) is slightly more complicated. We have obtained the next solution of a differential equation with the boundary conditions (u(R)=0, u'(0)=0):

$$u[r] = \frac{R^2\left(\frac{dp}{dx}\right)\left(-\text{BesselI}\left[0, M\right] + \text{BesselI}\left[0, \frac{Mr}{R}\right]\right)}{M^2\mu\,\text{BesselI}\left[0, M\right]}. \tag{2. 12}$$

$$\mathrm{u_b} = \frac{1}{\pi R^2}\int_0^R u\,2\pi r dr = \frac{R^2\left(\frac{dp}{dx}\right)\text{BesselI}\left[2, M\right]}{M^2\mu\,\text{BesselI}\left[0, M\right]}. \tag{2. 13}$$

Turbulent flow

In the case of turbulent flow, the logarithmic distribution of velocity that is the most suitable is, according to experimental work, the following:

$$\frac{u}{u^*} = \frac{1}{\kappa}ln\frac{(R-r)\rho u^*}{\mu} + B. \tag{2. 14}$$

With the upper equation, we could calculate the mean velocity in the circular channel for turbulent flow [7,8]:

$$u_b = \frac{1}{\pi R^2}\int_0^R\left(\frac{1}{\kappa}ln\frac{(R-r)\rho u^*}{\mu} + B\right)2\pi r dr =$$

$$\frac{1}{2}u^*\left(\frac{2}{\kappa}ln\frac{R\rho u^*}{\mu} + 2B - \frac{3}{\kappa}\right). \tag{2. 15}$$

In the presented model, we used the following values: $\kappa = 0.41$ and B=5.

3 VIBRATION OF PIPELINES

The equation of beam vibration containing flowing fluid could be written with the next equation, *[9-13]*:

$$EI\frac{\partial^4 z}{\partial x^4} = -\rho v^2 \frac{\partial^2 z}{\partial x^2} - 2\rho v \frac{\partial^2 z}{\partial x \partial t} - m\frac{\partial^2 z}{\partial t^2}. \tag{3. 1}$$

Equation (3. 1) is obtained with continuous vibration theory. In equation (3. 1) the v means the average fluid velocity, ρ the mass of fluid per unit length, E the modulus of elasticity, and I the moment of inertia, *[10-12]*. The first term is the force caused by the change in direction of the velocity of the fluid due to the curvature of the pipe. The second term is the force associated with the Coriolis acceleration, and the last term represents the force that is related to the vertical acceleration of the pipe.

For the simply supported pipeline, we obtain the next solution of the differential equation, *[9-12]*:

$$\frac{32\rho v\omega}{3l\left[EI\left(\frac{\pi}{l}\right)^4 - \rho v^2\left(\frac{\pi}{l}\right)^2 - m\omega^2\right]} = \frac{3l\left[EI\left(\frac{2\pi}{l}\right)^4 - \rho v^2\left(\frac{2\pi}{l}\right)^2 - m\omega^2\right]}{8\rho v\omega}. \tag{3. 2}$$

In equation (3. 2), ω means the angular velocity of the pipe relative to its length, and l the length between supports. With equation (3. 2), the relation between v and ω is expressed.

If we limit $\omega \Rightarrow 0$, equation (3. 3) calculates the critical velocity at which static divergence occurs:

$$v_c = \sqrt{\frac{EI\pi^2}{\rho l^2}}. \tag{3. 3}$$

4 RESULTS AND VIBRATIONAL ANALYSIS

Figure 3 shows analytical results for crude oil SAE 15W-40 flow at 200C through the pipeline with the next data: D=0.2m, μ=0.287 Pas, ϱ=878.7 kg/m³. The fluid flow is also turbulent at small pressure differences. Figure 4 shows analytical results for crude oil flow through the pipeline with the following data: D=0.002m, μ=0.287 Pas, ϱ=878.7 kg/m³. The fluid flow is also laminar at high-pressure differences.

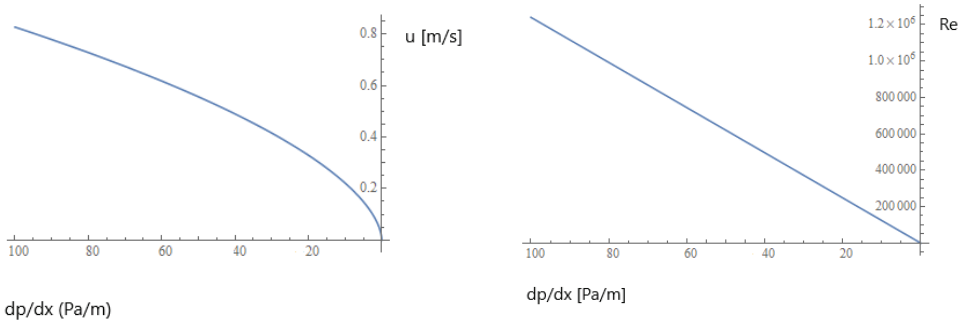

Figure 3: *Mean pipe velocity and Reynolds number developed by the turbulent model*

.

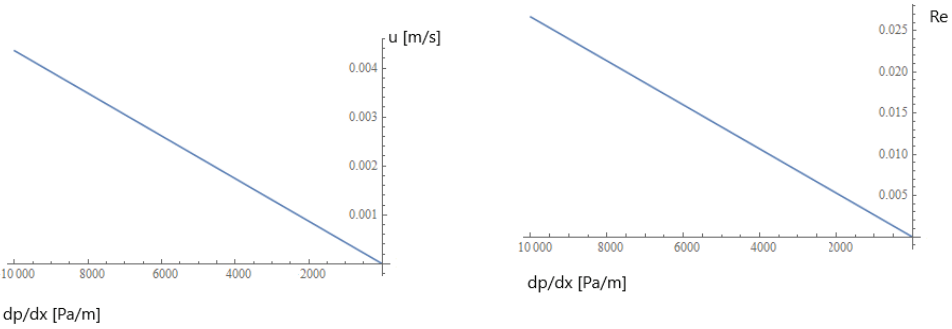

Figure 4: *Mean pipe velocity and Reynolds number developed by laminar fluid model*

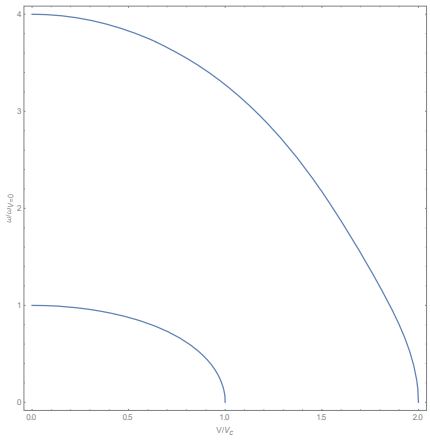

Figure 5: *Vibrational characteristics for steel pipeline containing crude oil (D=0.2m, μ=0.287 Pas, ϱ=878.7 kg/m³, δ=0.02m, L=10 m)*

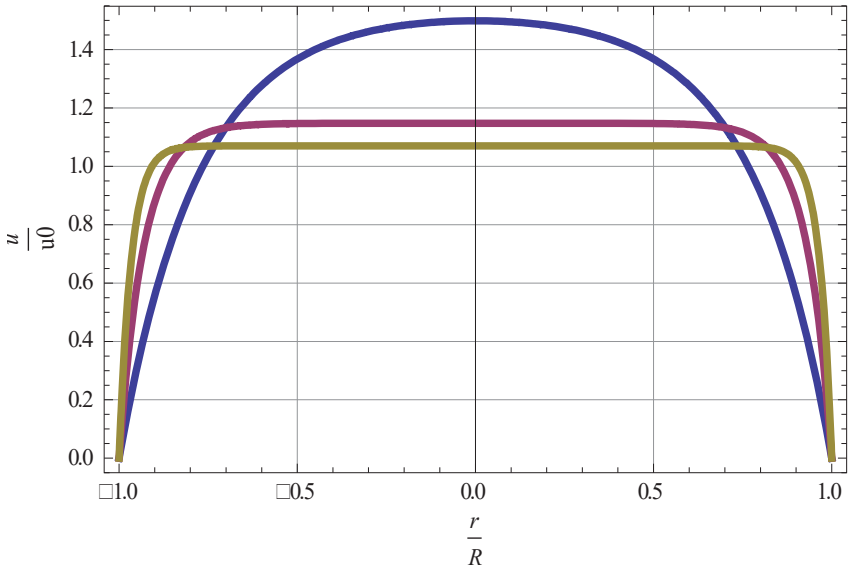

Figure 6: *Velocity profile with slip (β*=0.5) at M_H=5 (blue line), M_H=10 (red line) and M_H=30 (green line)in circular minichannel without slip*.

The analysis shows the velocity profile of crude oil in the pipeline. The inner diameter of the pipeline is in the first case 0.2 m in the second case 0.002 m. In the pipeline with diameter 0.2 m, the fluid flow is turbulent; in the pipeline with the diameter of 0.002 m, the fluid flow is laminar. Even more interesting are results for the calculation of natural frequencies for the first and second mode vibration regarding pipelines with crude oil. As we see from Figure 5, the natural frequencies of the pipe decrease as the fluid flow increases; from the figures, the influence of the average velocity profile in macro and mini-pipelines is also evident. Figure 6hows velocity profile for MHD flow in the circular channel.

5 CONCLUSION AND OUTLOOK

The present article shows the vibrational analysis of pipes conveying crude oil SAE 15W-40 flow. The fluid flow was calculated for laminar and turbulent flow. The vibrational characteristics have been calculated with vibration continuous pipeline theory.

References

[1] **V. Singhal, S. Garrimela, A. Raman:** *Microscale pumping technologies for microchannel cooling systems*, Appl. Mech. Rev., Vol. 57: 191-222, 2015

[2] **H. Chen:** *Vibration of a Pipeline Containing Fluid Flow with Elastic Support*, MsC Thesis, Ohio University, 1991

[3] **S. Rao:** *Vibration of continous systems*, Wiley, 2007

[4] **G. F. Naterer, O. B. Adeyinka:** *Microfluidic Exergy Loss in a Non-Polarized Thermomagnetic Field*, International Journal of Heat and Mass transfer, Vol. 48: 3945-3956, 2005

[5] **G. D. Ngoma, E. Erchiqui:** *Heat Flux effects on Liquid Flow in a Microchannel*, International Journal of Thermal Sciences, Vol. 46: 1076-1083, 2007

[6] **H. P. Mazumdar, U. N. Ganguly, S. K. Vanketesan:** *Some Effects on Magnetic Field on the Flow of a Newtonian Fluid through a Circular Tube*, Indian J. of Pure Applied Mathematics, 1996, Vol. 27: 519-524, 1996

[7] http://www.roymech.co.uk/Related/Fluids/Fluids_Viscosities.html

[8] **NPTEL:** *Principles of fluid mechanics*, http://nptel.ac.in/courses/101103004/

[9] **H. Dodds, H. L. Ruanyan:** *Effect of high velocity fluid flow on the bending vibrationsnand static divergence of a simply supported pipe*, NASA TN D-2870, 1965

[10] **H. Chen:** *Vibration of a pipeline containing fluid flow with elastic support*, Master science thesis, Ohio University, 1991

[11] **M. P. Paidoussis, S. J. Price, E. Langre:** Fluid structure interactions, Cambridge Press, 2010

[12] **R. D. Blevins:** *Flow-Induced Vibration*, Van Nostrand Reinhold, 1990

JET Journal of Energy Technology

JET Volume 12 (2019) p.p. 41-54
Issue 1, April 2019
Type of article 1.01
www.fe.um.si/en/jet.html

PANTOGRAPH DRIVEN WITH A LINEAR INDUCTION MOTOR WITH ADAPTIVE FUZZY CONTROL

PANTOGRAF GNAN Z LINEARNIM INDUKCIJSKIM MOTORJEM S PRILAGOJENIMI KRMILNIMI TEHNIKAMI

Costica Nituca[1], Gabriel Chiriac [1, ℜ]

Keywords: Linear induction motor, Fuzzy control, Locomotive pantograph, Simulation

Abstract

This article presents an adaptive fuzzy control for a linear induction motor, which is used to control the vertical movement of a pantograph, which supplies an electric locomotive from a contact line. The system has the goal of eliminating all the discontinuity on the route, the resonance phenomenon, the separation of the pantograph head from the contact wire, and electric arches. The simulations demonstrate functional control of the pantograph driven with a linear induction motor system using fuzzy control techniques.

Povzetek

V članku je predstavljeno prilagodljivo mehko krmiljenje linearnega indukcijskega motorja, ki se uporablja za krmiljenje navpičnega gibanja odjemnika toka, ki napaja električno lokomotivo iz kontaktne linije. Cilj sistema je odpraviti vse prekinitve na poti, resonančni pojav, ločitev glave odjemnika toka od kontaktnega vodnika in električnih lokov. Simulacije prikazujejo funkcionalno kontrolo odjemnika toka, ki se poganja z linearnim indukcijskim motornim sistemom z uporabo mehkih krmilnih tehnik.

ℜ Corresponding author: Ph.D. Gabriel Chiriac, Tel.: +04 0727 645058, Mailing address: Bd. Dimitrie Mangeron, nr. 21- 23, 700050 IASI, Romania, E-mail address: gchiriac@tuiasi.ro

[1] Technical University "Gheorghe Asachi" from Iasi, Faculty of Electrical Engineering, Bd. Dimitrie Mangeron, nr. 21- 23, 700050 IASI, Romania

1 INTRODUCTION

A critical problem of the electric supply of a high-speed locomotive is maintaining the contact force between the pantograph head and the contact line as constant and pursuing the trajectory of the contact point *[1, 2]*. The dynamic of the pantograph under the influence of the disruptive factors and perturbations is the decisive criteria in the estimation of the energy transfer quality from the contact line to electric vehicles. The contact line (the catenary) and the power supply system of the train (the pantograph) are in a highly dynamic interaction, which is influenced by the speed, the vehicle type, the structure of the catenary and the mechanical tension in the wire, the weather conditions, the structure and the mass of the pantograph and the oscillations and perturbations of the vehicle while moving.

The conventional methods to drive the pantograph use systems with compressed air or with springs. The control system can be based on different actuator types (hydraulic, pneumatic, electric), and for different actuator positions (strips suspension, air spring, or frame).

The use of the active control strategies for the pantograph *[3, 4]* may lead to an improvement of contact *[5]*. New mathematical models for the pantograph-catenary interaction have been developed in *[6, 7]*, as the basis for the control principles. The pantograph-catenary system is also analysed by using the finite element method *[8-11]*, the results being compared with results from the real tests. The damper system of the catenary is analysed by recording the accelerations of the pantograph *[12]*, while in *[13]* a control is proposed to reduce the oscillations of the pantograph-catenary system. The advanced active control of the pantograph includes the analysis of the vertical body vibration, as in *[14]*. According to *[15]*, the proposed controller can improve the contact quality, leading to a reduction of the standard deviation of the pantograph-catenary contact force by more than 40% compared to the non-controlled system.

The drive and the control of the pantograph head trajectory can be made by using a linear induction motor *[16]*. The patent *[16]* relates to a pantograph current collector to be used in locomotives or electric trains, for collecting power from an electric contact line placed along the railway. In addition to the mechanical resort that develops a lifting force and a force for pressing the contact shoe against the contact wire, the pantograph is provided with a supplementary assembly of a linear induction motor providing a supplementary mechanical effort, which is to be added to the mechanical effort achieved by a mechanical resort in order to adapt the resulting effort intended to push the pantograph's shoe. Thus, in parallel with the elastic spring of the pantograph or even independently, a linear induction motor that drives the pantograph head with the aim of pursuing the geometry of the contact line can be used. The linear motor can be controlled with the adaptive fuzzy control technique. Different articles have examined the fuzzy control approach for dynamics of the pantograph-catenary interaction *[17, 18]* and for the linear induction motors *[19-23]*.

This article presents the fuzzy adaptive control for a pantograph driven by a linear induction motor system used to supply an electric locomotive from a contact line. A mathematical model of the motor and the methodology for the motor control are presented. Simulations are made in Matlab-Simulink software, and data analyses are discussed.

2 PANTOGRAPH DRIVEN WITH A LINEAR INDUCTION MOTOR – SYSTEM DESCRIPTION

The main characteristic of a railway pantograph is to assure good current collecting, without interruptions of the current, regardless of the height of the pantograph and train movement. For this, it is necessary for the pantograph to have a permanent contact, regardless of the movement of the mechanically articulated system, as well as good lateral and transversal stability, to achieve contact pressure, regardless of the height in static and dynamic conditions.

The proposed solution is to use a linear induction motor (LIM) to drive the pantograph, a solution that is patented. Using this solution *[16],* (Figure 1), pantograph detachments will be prevented, and the electric traction equipment will be supplied in good conditions.

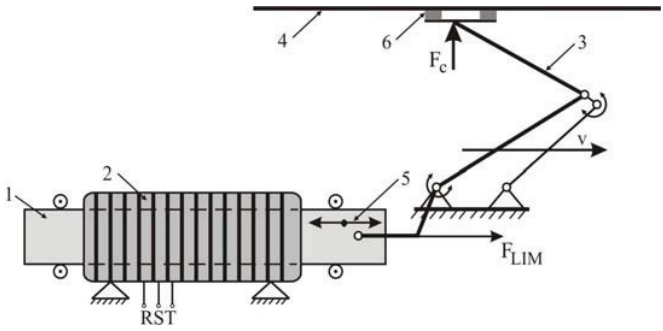

Figure 1: *Pantograph driven by a linear induction motor*

The linear induction motor (LIM) is three-phased and composed of a mobile plate armature (1) and two fixed inductors (2) with windings placed in 24 slots. The mobile armature is connected to the railway pantograph (3) and acts over it with force F_{LIM}. The pantograph pushes the contact line (4) with a contact force F_c. The mobile armature has a maximum oscillation motion (5) of 140 mm. The contact is assured by the skates (6).

3 MODEL OF THE SYSTEM

3.1 Model of the linear induction motor (LIM)

The dynamic model of the linear induction motor can be described with the following equations *[21, 24, 25]*:

$$\begin{cases} \dot{i}_{qs} = -\left(\dfrac{R_s}{\sigma \cdot L_s} + \dfrac{1-\sigma}{\sigma \cdot T_r}\right) \cdot i_{qs} + \dfrac{L_m}{\sigma \cdot L_s L_r T_r} \cdot \Phi_{qr} - \dfrac{n_p L_m \pi}{\sigma \cdot L_s L_r \tau} \cdot v\Phi_{dr} + \dfrac{1}{\sigma \cdot L_s} V_{qs}; \\ \dot{i}_{ds} = -\left(\dfrac{R_s}{\sigma \cdot L_s} + \dfrac{1-\sigma}{\sigma \cdot T_r}\right) \cdot i_{ds} + \dfrac{n_p L_m \pi}{\sigma \cdot L_s L_r \tau} \cdot v\Phi_{qr} + \dfrac{L_m}{\sigma \cdot L_s L_r T_r} \cdot \Phi_{dr} + \dfrac{1}{\sigma \cdot L_s} V_{ds}; \\ \dot{\Phi}_{qr} = \dfrac{L_m}{T_r} i_{qs} - \dfrac{1}{T_r} \Phi_{qr} + n_p \dfrac{\pi}{\tau} v\Phi_{dr}; \\ \dot{\Phi}_{dr} = \dfrac{L_m}{T_r} i_{ds} - n_p \dfrac{\pi}{\tau} v\Phi_{qr} - \dfrac{1}{T_r} \Phi_{dr}; \\ F_e = K_f \left(\Phi_{dr} i_{qs} - \Phi_{qr} i_{ds}\right). \end{cases} \tag{3.1}$$

where: $T = L_r/R_r$ is the time constant for the secondary circuit of the LIM;

$\sigma = 1 - \left(\dfrac{L_m^2}{L_s L_m}\right)$, dispersion coefficient of the LIM;

$K_f = \dfrac{3 n_p \pi L_m}{2 \tau L_r}$, is constantly used in the formula of the linear induction motor force, F_{LIM}.

3.2 The model of the pantograph – linear induction motor system

The mechanical equilibrium equation can be written as *[20]*:

$$F_e - F_r = M \frac{dv}{dt} = -Mv \frac{ds}{dt}. \tag{3.2}$$

The resistant force F_r is the necessary force to lift and to maintain the pantograph at the optimal height to follow the trajectory of the contact line (which is supposed to be sinusoidal) and to assure a constant contact force. Thus, the pantograph will have some vertical oscillations along the contact line and during the vehicle movement. It will be considered as positive (+) for the lift motion and negative (-) for the down motion *[26].*

To compensate these oscillations movements and to assure a constant contact force, the linear induction motor will operate as an electromagnetic resort *[16]* having a short oscillating movement and a relatively low speed. The resistant force is given by the equation:

$$F_r = \pm \mu_0 \frac{P_0 d_0}{2} \pm M_0 \omega^2 y \tag{3.3}$$

The pantograph-linear induction motor system will be described by the mechanical equilibrium equation, *[21, 22]*:

$$F_e = K_f \left(\Phi_{dr} i_{qs} - \Phi_{qr} i_{ds}\right) = M\dot{v} + Dv + F_r. \tag{3.4}$$

4 CONTROL METHODOLOGY FOR THE LINEAR INDUCTION MOTOR

Figure 2 presents the position control system for the linear induction motor *[19, 23, 24]*, with the following parameters:

$$F_e = K_f u_T \tag{4.1}$$

$$H_p(s) = \frac{1}{Ms + D} = \frac{b}{s + a} \tag{4.2}$$

where: $H_p(s)$ - transfer function of the motor; u_T - control signal; s- Laplace operator; a, b – constants.

In Figure 2, the parameter d_m is the desired position, and the parameter v_m is the desired speed.

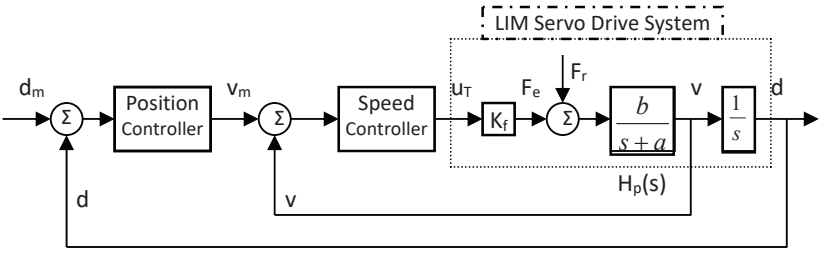

Figure 2: *Simplified position control system*

To obtain the control signal, a fuzzy adaptive regulator is proposed *[26]*.

4.1 Fuzzy adaptive regulator

The design of the fuzzy adaptive regulator is based on the aspects developed into the specific literature *[27-31]*. Hence, in this article, only the necessary steps to implement the fuzzy adaptive regulator are presented using Matlab-Simulink software. In Figure 3, a schematic for the fuzzy adaptive regulator is presented *[27, 28]*.

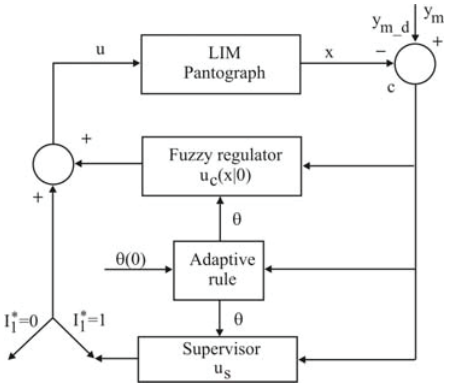

Figure 3: *Schematic of the fuzzy adaptive regulator*

Considering the signal u_c as a fuzzy system, the fuzzy adaptive regulator is designed as follows:

Step 1: *Preprocessing [27, 28].* There are specify $k_1,\ldots,k_n$ so that all the roots of the equation $s^n + k_1 s^{n-1} + \cdots + k_n = 0$ to be in the open left half plane. The positive definite *n x n* matrix *Q* is specified. The Lyapunov equation $\Lambda_c^T P + P\Lambda_c = -Q$, *Q*>0 is solved to obtain a symmetrical matrix *P*>0. The design parameters M_θ, M_x and σ are described based on practical constraints.

Step 2: Initial controller design *[28, 29]*:

u_c as a fuzzy system is considered.

$$u_c(\underline{x}|\underline{\theta}) = \frac{\sum_{i=1}^{M} \overline{y^l} \left[\prod_{i=1}^{n} \exp\left(-\left(\frac{x_i - \overline{x}^l}{\sigma_i^l} \right)^2 \right) \right]}{\sum_{i=1}^{M} \left[\prod_{i=1}^{n} \exp\left(-\left(\frac{x_i - \overline{x}^l}{\sigma_i^l} \right)^2 \right) \right]}; \tag{4.3}$$

where θ represents some adjustable parameters $\overline{y}^l$, $\overline{x}_i^l$ and σ_i^l.

The command u_c is designed according to the relation (4.3) based on *M* rules characterized by the Gaussian membership functions:

$$\mu_{F_i^l}(x_i) = \exp\left(-\left(\frac{x_i - \overline{x}^l}{\sigma_i^l} \right)^2 \right); \tag{4.4}$$

where *l* = 1,2,…,M and *i*= 1,2 …n.

Step 3. Design of the adaptive block *[27-29]:*

With the next algorithm, the relation $\frac{\partial u_c(\underline{x}|\underline{\theta})}{\partial \overline{y}^l}$ is derived:

$$\frac{\partial u_c}{\partial \overline{y}^l} = \frac{b^l}{\sum_{i=1}^{M} b^l}, \tag{4.5}$$

$$\frac{\partial u_c}{\partial \overline{x}_i^l} = \frac{\overline{y}^l - u_c}{\sum_{i=1}^{M} b^l} b^l \frac{-2\left(x_i - \overline{x}_i^l \right)}{\left(\sigma_i^l \right)}, \tag{4.6}$$

$$\frac{\partial u_c}{\partial \sigma_i^l} = \frac{\overline{y}^l - u_c}{\sum_{i=1}^{M} b^l} b^l \frac{-2\left(x_i - \overline{x}_i^l \right)^2}{\left(\sigma_i^l \right)^3}; \tag{4.7}$$

where:

$$b^l = \prod_{i=1}^{n} \exp\left(-\left(\frac{x_i - \bar{x}^l}{\sigma_i^l} \right)^2 \right). \tag{4.8}$$

The above relations are obtained considering the equations in (4.3) and the control u_s is given by *[13, 17]:*

$$u_s(\underline{x}) = I_1^* \operatorname{sgn}\left(\underline{e}^T P \underline{b}_c\right) \cdot \left[\left|u_c\right| + \frac{1}{b_L}\left(f^U + \left|y_m^{(n)}\right| + \left|\underline{k}^T \underline{e}\right|\right)\right], \tag{4.9}$$

where: $I_1^* = 1$ if $V_e > \bar{V}$ and $I_1^* = 0$ if $V_e \le \bar{V}$ *[15, 16]*.

The control *u* (Figure 3) is applied *[14, 15]*:

$$u = u_c(\underline{x}|\underline{\theta}) + u_s(\underline{x}), \tag{4.10}$$

where u_c is given by the relation (4.3) and u_s is given by the relation (4.9).

To adjust the vector $\underline{\theta}$, the next adaptive law is used:

if $\sigma_i^l = \sigma$, the following equation is used:

$$\dot{\sigma}_i^l = \begin{cases} \gamma \underline{e}^T \underline{p}_n \dfrac{\partial u_c}{\partial \sigma_i^l} & if \quad \underline{e}^T \underline{p}_n \dfrac{\partial u_c}{\partial \sigma_i^l} < 0 \\ 0 \quad if \quad \underline{e}^T \underline{p}_n \dfrac{\partial u_c}{\partial \sigma_i^l} \ge 0 \end{cases}; \tag{4.11}$$

Otherwise, the following equation is used:

$$\dot{\underline{\theta}} = \begin{cases} \gamma \underline{e}^T \underline{p}_n \dfrac{\partial u_c}{\partial \sigma_i^l} & if \quad \left(\left|\underline{\theta}\right| < M_\theta\right) \quad or \quad \left(\left|\underline{\theta}\right| = M_\theta \quad and \quad \underline{e}^T \underline{p}_n \underline{\theta}^T \dfrac{\partial u_c}{\partial \sigma_i^l} \ge 0\right) \\ \gamma \underline{e}^T \underline{p}_n \dfrac{\partial u_c}{\partial \sigma_i^l} - \gamma \underline{e}^T \underline{p}_n \dfrac{\underline{\theta}\underline{\theta}^T}{\left|\underline{\theta}\right|^2} \dfrac{\partial u_c}{\partial \underline{\theta}} & if \quad \left(\left|\underline{\theta}\right| = M_\theta \quad and \quad \underline{e}^T \underline{p}_n \underline{\theta}^T \dfrac{\partial u_c}{\partial \sigma_i^l} < 0\right) \end{cases}. \tag{4.12}$$

5 SIMULATIONS AND DATA ANALYSIS

For the simulations, a three-phased, bilateral, linear induction motor is used; it has the following parameters: V_F = 230V; I_f = 5A; R_s = 5.3Ω; R_r = 13.8Ω; L_m = 0.037H; L_r = 0.041H; L_s = 0.051H; K_f = 231.15 N/A; a = 23.741 ; b = 0.319; D = 57.1 kg/s; F_e = 150N; M = 12kg; v = 3m/s; τ = 0.027. The contact line considered for the simulations has the following parameters: span is 60m, deflection is 0.454m. The main pulsation of the contact line for a locomotive speed of 100km/h is ω = 2.907 1/s. Figure 4 presents the Matlab-Simulink schematic for the fuzzy adaptive regulator.

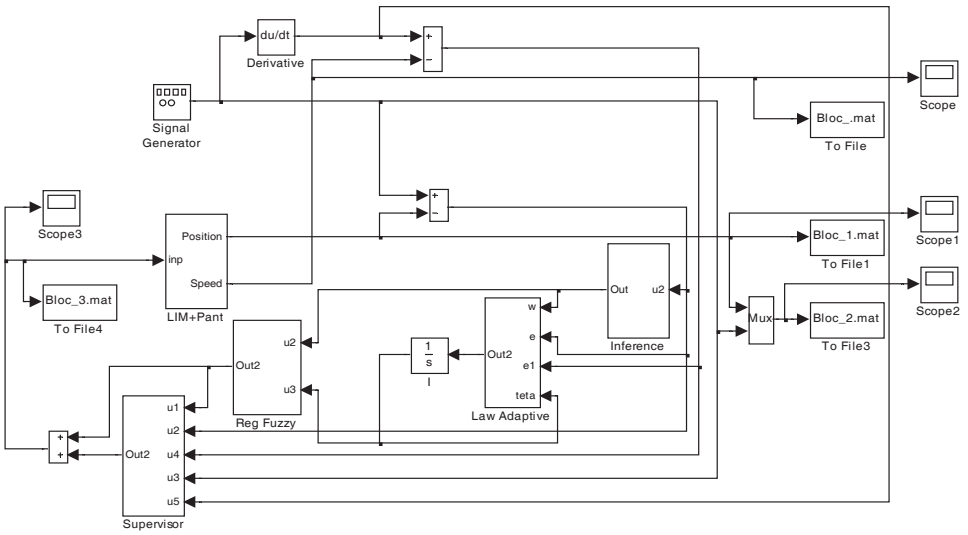

Figure 4: *Matlab-Simulink schematic for the fuzzy adaptive regulator*

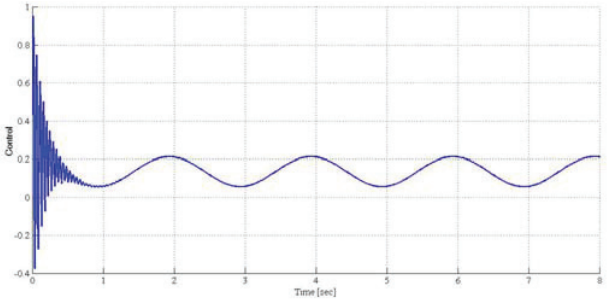

Figure 5: *Control signal variation*

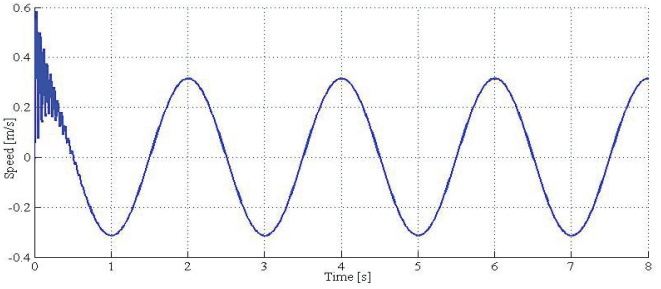

Figure 6: *Speed variation of the linear induction motor*

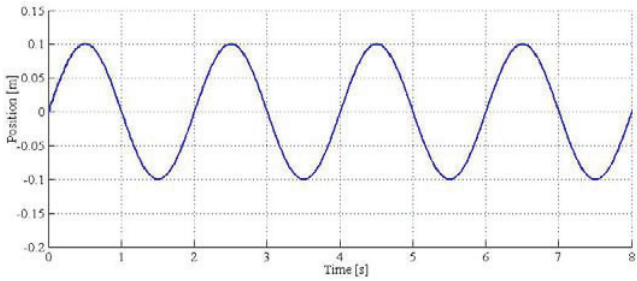

Figure 7: *Mobile armature motion (motor position)*

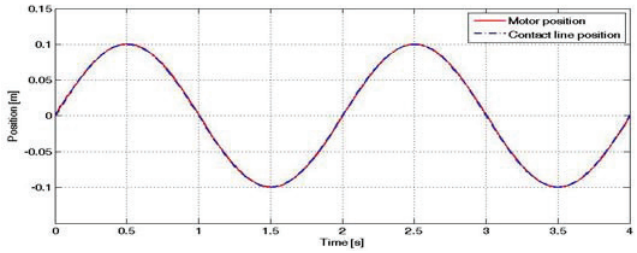

Figure 8: *Motor's movement and contact line position*

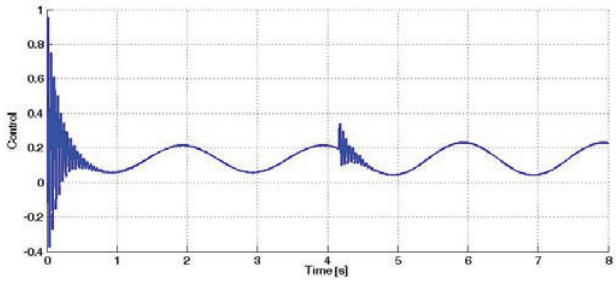

Figure 9: *Control signal variation with a supplementary, incidental force*

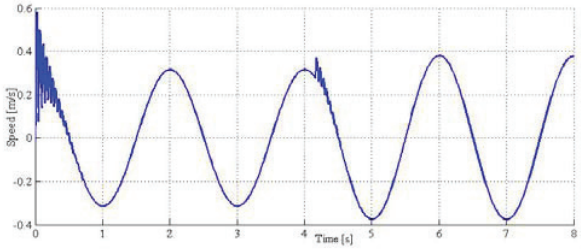

Figure 10: *Speed variation of the linear induction motor with supplementary, incidental force*

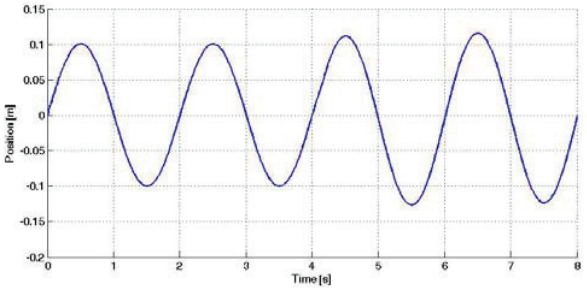

Figure 11: *Mobile armature motion (motor position) in case of the incidental force*

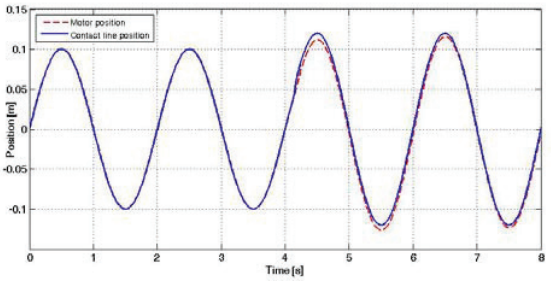

Figure 12: *Motor's movement and contact line position in case of the incidental force*

Figures 5 to 12 present the simulations of the pantograph driven by the linear motor system using a fuzzy adaptive regulator. Figure 5 presents the variation of the control signal, and Figure 6 presents the speed variation of the LIM and, accordingly, the vertical speed variation of the pantograph. The speed of the system has a variation of ±0.314 m/s.

Figure 7 presents the movement of the mobile armature (the plate) of the LIM, of the ±0.100 m. These variations are in accordance with the prescribed values of ±0.454 m.

Figure 8 presents the movement of the motor (red curve) and the position of the contact line (blue, dash curve) which must be followed by the pantograph. It can be observed that the two curves are very close, with differences of about (±0.1m), which demonstrate good control of the pantograph – linear motor system.

To estimate the operability of the system, a simulation for the overload was made, for the situation when the motor has to overcome a supplementary effort. For the simulation, the previous parameters are used, but, currently, a supplementary, incidental force is considered F_{1p}=20N.

Figure 9 describes the control signal with supplementary, incidental force F_{1p} at the moment t=4.16s, a force that modifies the shape of the control signal.

In Figure 10, the speed of the motor is depicted, with variations of ±0.314m/s in the first part of the simulation. When the supplementary force F_{1p} occurs, the variation speed becomes ±0.378m/s, with an increase of about 16%.

In Figure 11, it is observed that the variation of the position of the motor. When the supplementary force occurs, the position is modified from ±0.100m la ±0.117m.

Figure 12 shows the trajectory of the pantograph over the contact line when an incidental force appears. Thus, after the time t=4.163s, an increase also observed for the movement of the pantograph (red curve, ±0.1116m) and for the trajectory of the contact line (blue, dash curve, 0.12m). The difference between the two characteristics is of 0.0084m, which is about 7%; even in this situation, the system operates in the necessary conditions of the deflection of 0.454m.

6 CONCLUSIONS

Assuring continuous power collection for railway vehicles is essential for a safe transportation system. Problems regarding power collection are related to the pantograph detachment from the contact line due to the oscillations and parasitic movement of the vehicles and their power-collecting equipment. In this article, a solution to improve the power supply of the electric locomotive by using a linear induction motor to drive the pantograph is presented and analyzed. A mathematical model for the linear induction motor and the motor-pantograph system are developed, considering a fuzzy control technique. Simulations are made for two cases, with and without supplementary incidental force acting over the pantograph. The speed and position of the pantograph are discussed. Furthermore, the trajectory of the pantograph head in concordance with the trajectory of the contact line is also analysed. The simulations demonstrate good control of the pantograph-linear induction motor system using a fuzzy control technique.

References

[1] **S. Walters, A. Rachid, A. Mpanda:** *On Modelling and Control of Pantograph Catenary Systems,* In: PACIFIC 2011, Amiens, France, 2011

[2] **C. Nituca, A. Rachid, L. Cantemir, G. Chirac, Alina Gheorghiu**: Constructive and experimental aspects regarding the electric power collecting for very high speed traction, In The 6th International Conference on Electromechanical and power systems, Chişinău, October 2007

[3] **A. Collina, A. Facchinetti, F. Fossati***: An application of active control to the collector of an high-speed pantograph: simulation and laboratory tests*, Proc.of the 44th IEEE Conf. on Decision and Control, and European Control Conference 2005 Seville, Spain, pp. 4602-4609, 2005

[4] **R. Garg, P. Mahajan, P. Kumar**: *Effect of Controller Parameters on Pantograph-Catenary System*, American Int. J. of Research in Science, Technology, Engineering & Mathematics, 2(2), March-May, 2013, pp. 233-239

[5] **M**. **Carnevale**: *Innovative Solutions for Improving Pantograph Dynamics and Current Collection*, Ph. D. Thesis, Politecnico di Milano, Milan, Italy, 2011

[6] **A. Pisano, E**. **Usai**: *Contact force regulation in wire-actuated pantographs via variable structure control and frequency-domain techniques*, Int. J. of Control, vol. 81 (11), pp. 1747-1762, 2008

[7] **A. Rachid:** *Pantograph catenary control and observation using the LMI approach*, 50th IEEE Conf. on Decision and Control and European Control Conf. Orlando, USA, pp. 2287-2292, 2011

[8] **J.W. Kim, H.C. Chae, B.S. Park, S.Y. Lee,** et. al., *State sensitivity analysis of the pantograph system for a high-speed rail vehicle considering span length and static uplift force*. J. of Sound and Vibration vol. 303, pp. 405–427, 2007

[9] **Y.H. Cho:** *Numerical simulation of the dynamic responses of railway overhead contact lines to a moving pantograph considering a nonlinear dropper.* J. Sound and Vibration vol. 315, pp. 433–454, 2008

[10] **A. Collina, S. Bruni**: *Numerical Simulation of Pantograph-Overhead Equipment Interaction*, Vehicle System Dynamics, Vol. 38, No. 4, pp. 261-291, 2002

[11] **N. Zhou, W. Zhang**: *Investigation on dynamic performance and parameter optimization design of pantograph and catenary system,* Finite Elements in Analysis and Design vol. 47, pp. 288–295, 2011

[12] **P. Nåvik, A. Rønnquist, S. Stichel:** *Identification of system damping in railway catenary wire systems from full-scale measurements*, Engineering Structures, vol. (113), pp. 71–78, 2016.

[13] **S. Liu, L. Wu, X. Zhu**: *Researchof Pantograph–Catenary Active Vibration Control System Based on NARMA-L2 Model*, Proc. of 2015 Int. Conf. on Electrical and Information Technologies for Rail Transportation, Vol. 377, pp. 803-810, 12 March 2016

[14] **M.A. Abdullah, A. Ibrahim, Y. Michitsuji, M. Nagai:** *Active control of high-speed railway vehicle pantograph considering vertical body vibration*, Int. J. of Mechanical Engineering and Technology (IJMET), Vol. 4, Issue 6, pp. 263-274, November - December 2013

[15] **D. Guida, C. M. Pappalardo**: *Development of a Closed-Chain Multibody Model of a High-Speed Railway Pantograph for Hybrid Motion/Force Control of the Pantograph/Catenary Interaction,* Int. J. of Mechanical Engineering and Industrial Design, vol. 3(5), pp. 45-85, 2013

[16] **L. Cantemir, A. Rachid, C. Nituca, C.I. Barbanta, G. Chiriac, A.P. Alexandrescu:** Patent No. 128199/28.02.2018, OSIM, Romania, *Echipament de actionare electromagnetic a unui culegator de curent de tip pantograph*, 2018

[17] **Y.J. Huang:** *Discrete fuzzy variable structure control for pantograph position control, Electrical Engineering*, vol. 86.3, pp. 171-177, 2004

[18] **E. Karaköse, M.T. Gençoğlu:** *Adaptive fuzzy control approach for dynamic pantograph-catenary interaction*, In: *MECHATRONIKA, 15th International Symposium*, IEEE, pp. 1-5, 2012

[19] **F.J. Lin, R.J. Wai**: *Hybrid Control Using Recurrent Fuzzy Neural Network for Linear-Induction Motor Servo Drive,* IEEE Transactions on Fuzzy Systems, Vol. 9, No. 1, pp. 102-115, 2001

[20] **Gh. Livinţ, M. Petrescu, P. Livinţi**: *Modeling and control for linear induction motor electrical drive;* Buletinul Institutului Politehnic Iaşi, Tomul XLVIII, (LII), Fasc. 5, 2002

[21] **C.I Huang, K.C. Hsu, H.H. Chiang, K.Y. Kou, T.T. Lee**: *Adaptive Fuzzy Sliding Mode Control of Linear Induction Motors with Unknown End Effect Consideration*, Proceedings of the 2012 International Conference on Advanced Mechatronic Systems, Tokyo, Japan, September 18-21, pp. 626-631, 2012

[22] **M.A. Nasr Khoidja, M.A. Ouaz, B. Ben Salah, P. Brochet:** *Control of Velocity for a Linear Induction Motor***,** International Conference on Machine Intelligence, Tozeur – Tunisia, pp. 91-95, November 5-7, 2015

[23] **F.L. Lin, P.K. Huang, W.D. Chou**: *Genetic Algorithm Based Recurrent Fuzzy Neural Network For Linear Induction Motor Servo Drive*, Journal of the Chinese Institute of Engineers, Vol. 30, No. 5, pp. 801-817, 2007

[24] **I. Boldea, S.A. Nasar**: Linear Motion Electromagnetic Devices, Taylor & Francis November 5, 2001

[25] **R.J. Wai**: *Development of Intelligent Position Control System Using Optimal Design Technique*, IEEE Transactions on Industrial Electronics, vol. 50, no. 1, pp. 218-231, Feb. 2003

[26] **C. Nituca:** *Probleme de captare a curentului electric de la linia de contact pentru vehicule acţionate electric*, Universitatea Tehnică "Gheorghe Asachi" din Iaşi, 2003

[27] **L.X. Wang**: *Adaptive fuzzy systems and control: design and stability analysis*, Englewood Cliffs, N.J.: PTR Prentice Hall, 1994

[28] **L.X. Wang**: *A Course in Fuzzy Systems and Control*, Prentice Hall International Ed., 1996

[29] **L.X. Wang**: *Stable Adaptive Fuzzy Controllers with Application to Inverted Pendulum Tracking,* IEEE Transactions on Systems, Man, and Cybernetics-Part b: Cybernetics, vol. 26, no. 5, pp. 667-691, October 1996

[30] **F. Wan, L.X. Wang, Y. Sun**: *One-stepahead Adaptive Control for a General Class of Nonlinear Dynamic Systems based on Fuzzy Models*, Proceedings of the American Control Conference Arlington, VA, pp. 4782-4787, June 25-27, 2001

[31] **C.M. Lin, C.F. Hsu:** *Recurrent-Neural-Network-Based Adaptive-Backstepping Control for Induction Servomotors*, IEEE Transactions on Industrial Electronics, vol. 52, no. 6, pp. 1677- 1684, December 2005

Nomenclature

(Symbols)	(Symbol meaning)
d_0	diameter of the shaft load of the pantograph
D	viscous friction and iron-loss coefficient
F_e	electromagnetic force
F_r	external force disturbance
i_{qs}	q-axis primary current
i_{ds}	d-axis primary current
K_f	force constant
L_m	magnetizing inductance per phase
L_r	secondary inductance per phase
L_s	primary inductance per phase
M	total mass of the moving element
M_0	*t*otal mass of the pantograph related to the skate;
n_p	number of pole pairs
P_0	*t*he static equivalent load of the pantograph;
R_s	winding resistance per phase
R_r	secondary resistance per phase referred primary
T_r	secondary time-constant
v	mover linear velocity
V_{ds}	d-axis primary voltage
V_{qs}	q-axis primary voltage
y	amplitude of the catenary
σ	leakage coefficient
Φ_{dr}	d-axis secondary flux
Φ_{qr}	q-axis secondary flux
τ	pole pitch
μ_0	the friction coefficient in bearings
ω	catenary angular frequency

Journal of Energy Technology

JET Volume 12 (2019) p.p. 55-67
Issue 1, April 2019
Type of article 1.01
www.fe.um.si/en/jet.html

ENERGY INDICATORS AND TOPICS IN FOOD SUPPLY CHAINS' LIFE CYCLE ASSESSMENT

ENERGETSKI KAZALCI IN VSEBINE V CELOSTNEM VREDNOTENU OKOLJSKIH VPLIVOV PREHRAMBENIH OSKRBOVALNIH VERIG

Petra Vidergar[1], Rebeka Kovačič Lukman[1]✉

Keywords: energy, food supply chain, life cycle assessment, Leximancer

Abstract

Food supply chains have a significant impact on the environment, using large amounts of fossil energy resources and other non-renewable resources. Energy is directly and indirectly needed in all the steps along the food supply chain. This paper explores energy-related indicators in food supply chains and life cycle assessment within sixty-six research papers, gathered from the Web of Science database. Furthermore, a quantitative content analysis was carried out to assess the research trends and future opportunities regarding energy-related topics. The results revealed that a holistic perspective is needed, as energy-related indicators should be included in the use and end-of-life stages, not only in the production processes, and that the inclusion should follow the life cycle assessment methodology. The current research topics are energy issues related to production processes and environmental impacts. Improvements are possible in extending research areas to renewable resources, whole life-cycle perspectives, and socio-economic consequences.

✉1 Corresponding author: Assoc. prof. dr. Rebeka Kovačič Lukman, Mailing address: Mariborska c.7, SI-3000 Celje, E-mail address: rebeka.kovacic@um.si

[1] University of Maribor, Faculty of Logistic, Mariborska c.7, SI-3000 Celje

Povzetek

Prehrambene oskrbovalne verige pomembno vplivajo na okolje, saj v procesih uporabljajo veliko količino fosilnih goriv in drugih neobnovljivih virov. Energija je neposredno in posredno potrebna v vseh korakih prehrambene oskrbovalne verige. Članek obravnava energetske kazalnike v celostni oceni življenjskega cikla prehrambenih oskrbovalnih verig, in sicer v šestinšestdesetih raziskovalnih člankih, zbranih iz podatkovne baze Web of Science. Poleg tega smo izvedli kvantitativno vsebinsko analizo, da bi ocenili trende raziskav in priložnosti v prihodnosti. Rezultati so pokazali, da je potreben celovit pogled, saj bi morali biti energetski kazalniki vključeni v fazo uporabe in ob koncu življenjske dobe, ne le v proizvodnih procesih. Vključitev kazalcev za izračun kategorij vpliva bi morala slediti metodologiji celovitega ocenjevanja življenjskega cikla. Trenutne raziskovalne teme povezujejo energetske vsebine s proizvodnimi procesi in posledično vplivi na okolje. Izboljšave so možne pri razširitvi raziskovalnih področij na obnovljive vire, celotni življenjski cikel in družbeno-ekonomske vsebine.

1 INTRODUCTION

Food supply chains have huge impacts on the local and global environments, as they heavily depend on fossil fuel energy supply and other non-renewable resources, *[1]*. Energy is needed in all steps along the food supply chain: in the production of crops, fish, livestock and forestry products; in post-harvest operations; in food storage and processing; in food transport and distribution; and in food preparation. The direct and indirect energy used in the food supply chain is represented in Figure 1. Direct energy includes electricity, mechanical power, as well as solid, liquid, and gaseous fuels. Indirect energy refers to the energy required for manufacturing inputs such as machinery, farm equipment, fertilizers and pesticides, *[2].* The Food and Agricultural Organization of the United Nations (FAO), *[2]*, further argues that the energy type used in the food chain and the way it is used in large determine whether food systems can meet future food security goals and support broader development objectives in an environmentally sustainable manner, *[2].*

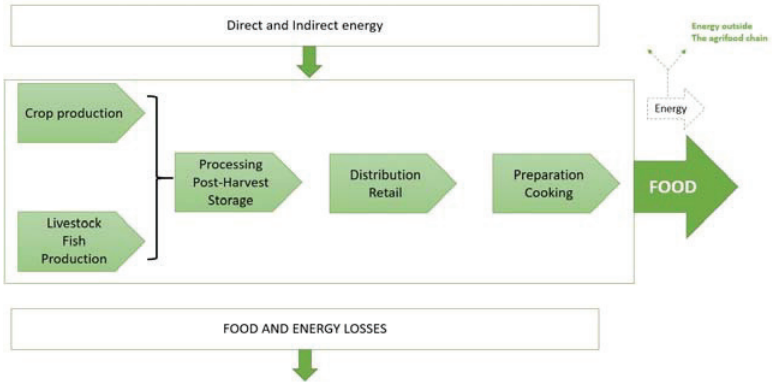

Figure 1: *Direct and indirect energy use in food supply chains (adapted from [2])*

As reported by the European Commission, the food sector contributes to 23 per cent global resource use and 31 per cent acidifying emissions, *[3].* Also, Noya et al., *[4]*, reported that a large amount of resources is required for food production and a great deal of food waste is

formed in food supply chains throughout the life cycle. Consequently, the food sector is responsible for around 20 per cent of greenhouse gas emissions, which are expected to expand in a correlation with the global food demand, *[5].* FAO, *[2]*, projections indicate that by 2050 a 70 per cent increase in food production over 2005-2007 levels will be necessary to meet the expanding demand for food. Therefore, the need for a transition from fossil to sustainable resource usage for a global food supply chain exists, *[6].* To approach the transition, an understanding of energy demand and resources usage related to the environmental impacts is a prerequisite, *[7].*

Life cycle assessment (LCA) is an approach that evaluates all the stages of a product's life. During this evaluation environmental impacts from each stage are considered, from raw material acquisition, processing to distribution and use, and finally disposal, recycling, etc. This methodology considers not only the material flows but also the outputs and their environmental impacts, *[8].* The LCA methodology was standardized with ISO 14040, *[9]*, and ISO 14044, *[10]*, and consists of the following main steps: goal and scope definition, inventory analysis, life cycle impact assessment and interpretation. As claimed by McAuliffe et al., *[11]*, LCA is considered to be one of the most informative tools to quantitatively compare environmental performances of multiple food consumption strategies. Arvidsson and Svanström, *[12]*, argue that many different energy indicators are used in LCA studies to account for energy issues in various ways, where their application and choices are poorly described.

The goal of this paper is two-fold. First, to obtain an in-depth view of the energy-related indicators in food supply chain LCA studies to assess their current state-of-the-art, usage, transparency and consistency. Second, to identify research areas and topics related to energy issues and LCA, by using quantitative content analysis to assess trends and opportunities in future research. Thus, sixty-six LCA food supply chain scientific papers, published from 2009 to 2019 were systematically reviewed and elaborated.

2 METHODS

Our research is based on scientific papers found in the Web of Science only, as it represents the most comprehensive scientific databased of publications with impact factors. For the search purposes keywords “LCA” and “food supply chain” were used. The review was carried out at the beginning of 2019. Conference papers, proceedings, and monographs were not considered, as our interest was identifying purely scientific publications with impact factors, which went through the strict and in-depth review process, assuring their novelty and added value to the scientific community. Two-hundred and forty-four such papers were identified. Reading titles, abstracts, and keywords revealed that not all are suitable to be included in our study as they included unrelated topics, for example, water supply, food packaging, and did not include LCA as such. Thus, we have ended up with sixty-six suitable papers, with which we have focused on energy indicators and quantitative content analysis.

When researching energy indicators in the existing LCA studies to identify the state-of-the-art, the illustration of the energy indicator generated by Arvidsson and Svanström, *[12]*, was considered as a framework. See Figure 2.

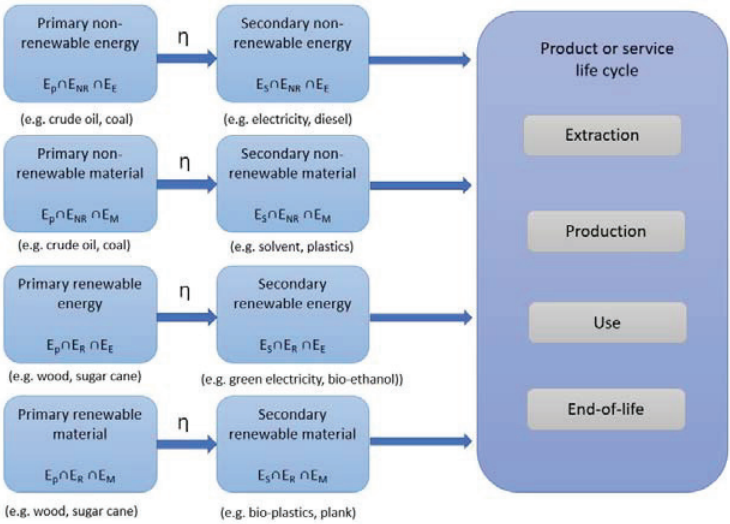

Figure 2: *A graphical illustration of the suggested framework for energy indicators in LCA, [12]*

The quantitative content analysis, including both thematic and semantic analyses, was carried out using Leximancer software, version 4.5, which can identify core concepts and their correlations. Leximancer uses statistical algorithms, integrating nonlinear dynamics and machine learning, enabling a quantitative content analysis by determining concepts' presence in textual documents, so manageable categories and relationships can be formed, *[13].* Consequently, a result is a concepts list with relationships visualized via a concept map, *[14].* The themes importance is expressed by the circles colour, where the "hottest" or most important theme appears in red, and the next "hottest" in orange, etc., according to the colour wheel. Concepts within the themes (coloured circles) are strongly related to the theme in which the concept is located. Another sign of importance is the circles' size (the size indicates how many concepts have been clustered together). The distance between concepts shows concepts relations, *[15]*, in which semantically less related concepts are mapped apart, while close concepts even overlap, *[16].* Baldauf and Kaplan, *[17]*, argued that the software is appropriate for exploratory research as it produces high concept extractions and thematic clustering reliability and reproducibility.

3 RESULTS

The results section represents the papers' analyses, including energy-related indicators and Leximancer's thematic and semantic results. Energy-related indicators were evaluated according to the framework Arvidsson and Svanström, *[12]*, which we have modified, see Table 1.

***Table 1**: Fraction (in %) of energy indicators and energy data used in LCA food supply chain*

Life cycle	Primary non-renewable energy	Secondary non-renewable energy	Primary renewable energy	Secondary renewable energy
Extraction	0	12	2	2
Production	0	100	4	19
Use	0	8	0	2
End-of-life	0	10	0	0

In the energy indicators and data search, we have identified fifty-two papers (out of sixty-six). Table 1 indicates that within the fifty-two papers, all contained the energy secondary non-renewable energy indicator, mostly calculated as electricity or diesel fuel used; 12% of the fifty-two papers considered secondary non-renewable energy, mostly in the cultivation of plants processes within the extraction phase. Jez et al., *[18]*, considered primary and secondary renewable energy by exploring oil production from micro-algae and terrestrial oilseed crops. Freon et al., *[19]*, compared the use of natural gas and fuel within fishmeal plants, while Miah et al., *[20]*, compared direct natural gas energy and indirect electricity energy. However, the authors did not consider primary non-renewable energy, and only 2% of the papers considered primary renewable energy indicators/data. Within the reviewed papers, the authors only briefly mention the energy considered in their calculations and do not specifically determine, which kind of energy data or indicators are included in the results. As indicated in Table 1, energy-related indicators or data mostly focused on the production processes.

Regarding the methodology and indicators, it is important to mention the third LCA step (i.e., LCIA), in which 20% of studies “energy impact category” emerged, e.g., primary energy demand, cumulative energy demand indicator (CED), non-renewable energy demand, etc., which is later discussed.

Sixty-six reviewed papers were examined using Leximancer software to determine the main concepts related to energy within the LCA food supply chain studies. Non-relevant words, such as “year”, “study”, “using”, “figure”, “table”, etc., were excluded. The concepts were then collected into themes (see Figure 3).

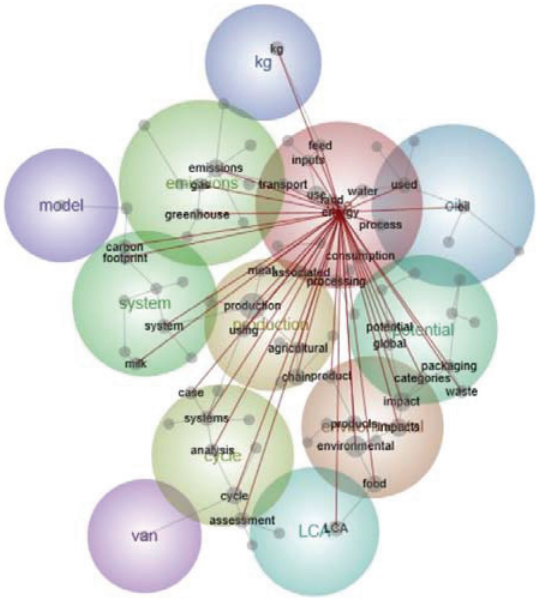

Figure 3: *Energy-related concepts*

The content analysis results indicated that *use*, *environment* and *production* are the most dominant themes, and the most dominant concept clusters within them (within individual circles) are "energy", "production", and "environmental impacts". Thus, the "energy" concept cluster covers "use", "consumption", "processes", "water", "inputs", "feed", and "transport", showing a close interlinkage between these concepts. Our main research topic was the energy-related issues in LCA of food supply chains; thus, a focus was given to the "energy" concept, see Figure 3 and its relations to other concepts. The "energy" concept is closely related to concepts of "production" and "environmental impacts".

Related Word-Like	Count	Likelihood
demand	1005	60%
inputs	617	25%
water	991	24%
consumption	1027	24%
efficiency	298	23%
materials	455	23%
use	1787	21%
gas	612	18%
greenhouse	364	17%
primary	262	17%
increase	241	17%
process	457	16%
land	393	16%
local	243	16%
associated	406	15%
reduce	231	15%
distribution	302	14%

Figure 4: *The "energy" concept ranking table*

To get a more in-depth view, we ran another analysis, the concept ranking table (see Figure 4), to explore and indicate the relevance of the concept (in %) and their likelihood. This represents a measure: a relative strength indicator of a concept's occurrence frequency. As shown in Figure 4, 60% of the text containing the concept "energy" also contains the concept "demand", and express a conditional probability if the data discuss "energy" then "demand" will also be mentioned, followed by concepts "inputs", "water", "consumption", and "use".

4 DISCUSSION AND CONCLUSIONS

In fifty-two papers out of sixty-six, we have identified energy-related indicators and data. The studies mostly cover production processes, identifying environmental impacts from electricity or diesel use (secondary non-renewable energy). Eight per cent of papers covered all the life cycle phases (extraction, production, use, and end-of-life), while primary non-renewable resources (crude oil, coal) were not considered. This shows that the system boundary for the studies was narrowed down and the cut-off criteria were employed. However, such narrowing processes might be uncertain in terms of comprehensiveness and transparency, as the FAO, *[2]*, claims that supply chains are highly dependent on fossil fuels, and could have a high impact on the obtained results. It is also interesting that authors did not consider renewable sources at the end-of-life-stage as materials, because other resources can be re-used, re-cycled, especially when considering principles of the circular economy.

Furthermore, twenty per cent of studies used energy-related indicators in the stage of LCIA as impact categories, which might also be arbitrary, from the LCA methodological perspective, as they are indicators, not the impact categories. Turconi, *[21]*, argued that impact categories should not be confused with lifecycle energy indicators such as CED (normally expressed as energy input per unit of product, i.e., kWh electricity), which is often used with power generation technologies to assess their performance. Also, Huijbregts et al., [22], states that CED can serve as a screening indicator for environmental performance, but its usefulness as a stand-alone indicator for environmental impact is very limited. Product environmental performance guides, *[23]*, further suggest that the identification of the most relevant impact categories shall be based on the normalized and weighted results, and at least three relevant impact categories (e.g., global warming, acidification, eutrophication, etc.) shall be considered; the results shall not be represented via one impact category or even one indicator.

Considering a quantitative content analysis, the energy theme emerged as significant within the LCA supply chain studies, which is expected as the food supply chain processes heavily depend on energy sources, directly and indirectly linked to all the life cycle stages; thus, energy demand emerged as most significant. The quantitative content analysis also revealed the main research areas: energy, production, and environmental impacts, which are also related, as LCA studies of the food supply chain evaluated production processes and their environmental impacts. However, the concept perspective of energy theme within the studies is limited by processes, consumption and transport. This opens up a need for an extension of research contents within the LCA, especially the importance of renewable resources, and end-of-life options (such as the circular economy) or various products' usage at the end-of-life. This will also assure a comprehensiveness of the LCA, not focusing only on the production stage. However, energy-related issues did not reveal any role of economic or societal related topics, the integration of which would be interesting.

To summarize, our study argues that including energy-related indicators is of utmost importance to obtain a holistic perspective. However, they should be more comprehensive, comprising (besides extraction and production stages) use and end-of-life, the data acquisition of which might be very demanding. Furthermore, indicators' inclusion should follow the LCA methodological rules, as suggested. We have identified that room for improvement exists within energy-related issues in the LCA food supply chain studies, embracing renewable resources, whole life-cycle perspective, and socio-economic topics.

References

[1] **M.V. Markussen, M. Kulak, L.G. Smith, T. Nemecek, H. Østergård:** *Evaluating the sustainability of a small-scale low-input organic vegetable supply system in the United Kingdom*, Sustainability, Vol. 6, Iss. 4, p.p. 1913-1945, 2014

[2] **Food and Agricultural Organization of the United Nations (FAO):** Energy-Smart Food at FAO: An overview. Chapter 1: At a glance: a role of energy in food security and climate, 2015. Available online: http://www.fao.org/3/an913e/an913e01.pdf (accessed: 10 April 2019).

[3] **J. Bengtsson, J. Seddon:** *Cradle to retailer or quick service restaurant gate life cycle assessment of chicken products in Australia,* Journal of Cleaner Production, Vol. 41, p.p. 291-300, 2013

[4] **L.I. Noya, V. Vasilaki, V. Stojceska, S. González-García, C. Kleynhans, S. Tassou, E. Katsou:** *An environmental evaluation of food supply chain using life cycle assessment: A case study on gluten free biscuit products*, Journal of Cleaner Production, Vol. 170, p.p 451-461, 2018

[5] **W.L. Biswas, G. Naude:** *A life cycle assessment of processed meat products supplied to Barrow Island: a Western Australian case study*. Journal of Food Engineering, Vol. *180*, p.p. 48-59, 2016

[6] **N. M Holden, E. P. White, M. C. Lange, T. L. Oldfield:** *Review of the sustainability of food systems and transition using the Internet of Food,* npj Science of Food, Vol. 2, Iss. 1, p.p. 18, 2018

[7] **S. Keyes,P. Tyedmers, K. Beazley:** *Evaluating the environmental impacts of conventional and organic apple production in Nova Scotia, Canada, through life cycle assessment,* Journal of Cleaner Production, Vol. 104, p.p 40-51, 2015

[8] **L. Mogensen, J.E. Hermansen, N. Halberg, R. Dalgaard**: *Life Cycle Assessment across food supply chain,* Sustainability in Food Industry. Chapter 5 p.p. 115–144. 2009.

[9] **International Organization for Standardization:** ISO, Environmental Management – life cycle assessment – principles and framework, ISO 14040, Geneva, 2006

[10] **International Organization for Standardization:** ISO, Environmental Management – life cycle assessment – principles and framework, ISO 14044, Geneva, 2006

[11] **G. A McAuliffe, T. Takahashi, M. R. Lee:** *Framework for life cycle assessment of livestock production systems to account for the nutritional quality of final products*, Food and energy security, Vol. 7, Iss. 3, e00143, 2018

[12] **R. Arvidsson, M. Svanström:** *A Framework for Energy Use Indicators and Their Reporting in Life Cycle Assessment.* Integrated Environmental Assessment and Management, Vol. 12, Iss. 3, p.p. 429–436, 2015.

[13] **D. Angus, S. Rintel, J. Wiles:** *Making sense of big text: a visual-first approach for analysing text data using Leximancer and Discursis*. International Journal of Social Research Methodology, Vol. 16, Iss. 30 p.p. 261-267, 2013

[14] **B. Hyndman, S. Pill:** *What's in a concept? A Leximancer text mining analysis of physical literacy across the international literature*. European Physical Education Review, Vol. 24, Iss. 3, p.p. 292-313, 2018

[15] **C. Biesenthal, R. Wilden:** *Multi-level project governance: Trends and opportunities.* International Journal of Project Management, Vol. 32 Iss. 8, p.p. 1291-1308, 2014

[16] **C. Campbell, L. F. Pitt, M. Parent, P. R. Berthon:** *Understanding consumer conversations around ads in a Web 2.0 world.* Journal of Advertising, Vol. 40, Iss. 1, p.p. 87-102, 2011

[17] **R. B. Baldauf, R. B. Kaplan:** *Australian applied linguistics in relation to international trends*. Australian Review of Applied Linguistics, Vol. 33, Iss. 1, p.p 4-1, 2010

[18] **S. Jez, D. Spinelli, A. Fierro, A. Dibenedetto, M. Aresta, E. Busi, R. Basosi:** *Comparative life cycle assessment study on environmental impact of oil production from micro-algae and terrestrial oilseed crops.* Bioresource technology, Vol. 239, p.p. 266-275, 2017

[19] **P. Fréon, H., Durand, A. Avadí, S. Huaranca, R. O. Moreyra:** *Life cycle assessment of three Peruvian fishmeal plants: Toward a cleaner production*. Journal of cleaner production, Vol. 145, p.p. 50-63, 2017

[20] **J. H. Miah, A. Griffiths, R. McNeill, S. Halvorson, U. Schenker, N. D. Espinoza-Orias, J. Sadhukhan:** *Environmental management of confectionery products: Life cycle impacts and improvement strategies*. Journal of cleaner production, Vol. 177, p.p. 732-751, 2018

[21] **R. Turconi**: Life cycle assessment of electricity systems. Kgs. Lyngby: DTU Environment. 2014. Available online: http://orbit.dtu.dk/files/89362197/Roberto_Turconi_PhD_Thesis_WWW_Version.pdf (accessed 10th April 2019).

[22] **M.A. Huijbregts, L. J.A. Rombouts, S. Hellweg, R. Frischknecht, J. A. Hendriks, D. van de Meent, A. M.J. Ragas, L. Reijnders, J. Struijs**: *Is Cumulative Fossil Energy Demand a Useful Indicator for Environmental Performance of Products*. Environ. Sci. Technol. Vol. 40, Iss. 3, p.p. 641–648, 2006.

[23] **European Commission**. PEFCR Guidance document, - Guidance for the 14 development of Product Environmental Footprint Category Rules (PEFCRs), version 6.3, May 2018.

APPENDIX

A list of papers included in our study.

Paper No.	Paper
1.	Arnal, Á., Royo, P., Pataro, G., Ferrari, G., Ferreira, V., López-Sabirón, A., & Ferreira, G. (2018). Implementation of PEF Treatment at Real-Scale Tomatoes Processing Considering LCA Methodology as an Innovation Strategy in the Agri-Food Sector. *Sustainability*, *10*(4), 979.
2.	Bengtsson, J., & Seddon, J. (2013). Cradle to retailer or quick service restaurant gate life cycle assessment of chicken products in Australia. *Journal of Cleaner Production*, *41*, 291-300.
3.	Biswas, W. K., & Naude, G. (2016). A life cycle assessment of processed meat products supplied to Barrow Island: a Western Australian case study. *Journal of Food Engineering*, *180*, 48-59.
4.	Bosona, T., & Gebresenbet, G. (2018). Life cycle analysis of organic tomato production and supply in Sweden. *Journal of cleaner production*, *196*, 635-643.
5.	Burek, J., Kim, D., Nutter, D., Selke, S., Auras, R., Cashman, S., ... & Thoma, G. (2018). Environmental sustainability of fluid milk delivery systems in the United States. *Journal of Industrial Ecology*, *22*(1), 180-195.
6.	Cecchini, L., Torquati, B., Paffarini, C., Barbanera, M., Foschini, D., & Chiorri, M. (2016). The milk supply chain in italy's umbria region: Environmental and economic sustainability. *Sustainability*, *8*(8), 728.
7.	Del Borghi, A., Gallo, M., Strazza, C., & Del Borghi, M. (2014). An evaluation of environmental sustainability in the food industry through Life Cycle Assessment: the case study of tomato products supply chain. *Journal of cleaner production*, *78*, 121-130.
8.	Depping, V., Grunow, M., van Middelaar, C., & Dumpler, J. (2017). Integrating environmental impact assessment into new product development and processing-technology selection: Milk concentrates as substitutes for milk powders. *Journal of Cleaner Production*, *149*, 1-10.
9.	Djekic, I., Sanjuán, N., Clemente, G., Jambrak, A. R., Djukić-Vuković, A., Brodnjak, U. V., ... & Tonda, A. (2018). Review on environmental models in the food chain-Current status and future perspectives. *Journal of cleaner production*, *176*, 1012-1025.
10.	Farmery, A. K., Gardner, C., Green, B. S., Jennings, S., & Watson, R. A. (2015). Domestic or imported? An assessment of carbon footprints and sustainability of seafood consumed in Australia. *Environmental Science & Policy*, *54*, 35-43.
11.	Farmery, A., Gardner, C., Green, B. S., Jennings, S., & Watson, R. (2015). Life cycle assessment of wild capture prawns: expanding sustainability considerations in the Australian Northern Prawn Fishery. *Journal of cleaner production*, *87*, 96-104.
12.	Fréon, P., Durand, H., Avadí, A., Huaranca, S., & Moreyra, R. O. (2017). Life cycle assessment of three Peruvian fishmeal plants: Toward a cleaner production. *Journal of cleaner production*, *145*, 50-63.
13.	Glew, D., & Lovett, P. N. (2014). Life cycle analysis of shea butter use in cosmetics: from parklands to product, low carbon opportunities. *Journal of cleaner production*, *68*, 73-80.

14.	Hessle, A., Bertilsson, J., Stenberg, B., Kumm, K. I., & Sonesson, U. (2017). Combining environmentally and economically sustainable dairy and beef production in Sweden. *Agricultural Systems*, *156*, 105-114.
15.	Ingrao, C., Licciardello, F., Pecorino, B., Muratore, G., Zerbo, A., & Messineo, A. (2018). Energy and environmental assessment of a traditional durum-wheat bread. *Journal of cleaner production*, *171*, 1494-1509.
16.	Jez, S., Spinelli, D., Fierro, A., Dibenedetto, A., Aresta, M., Busi, E., & Basosi, R. (2017). Comparative life cycle assessment study on environmental impact of oil production from micro-algae and terrestrial oilseed crops. *Bioresource technology*, *239*, 266-275.
17.	Keyes, S., Tyedmers, P., & Beazley, K. (2015). Evaluating the environmental impacts of conventional and organic apple production in Nova Scotia, Canada, through life cycle assessment. *Journal of Cleaner Production*, *104*, 40-51.
18.	Kim, D., Thoma, G., Nutter, D., Milani, F., Ulrich, R., & Norris, G. (2013). Life cycle assessment of cheese and whey production in the USA. *The International Journal of Life Cycle Assessment*, *18*(5), 1019-1035.
19.	Konstantas, A., Jeswani, H. K., Stamford, L., & Azapagic, A. (2018). Environmental impacts of chocolate production and consumption in the UK. *Food research international*, *106*, 1012-1025.
20.	Kulak, M., Nemecek, T., Frossard, E., & Gaillard, G. (2016). Eco-efficiency improvement by using integrative design and life cycle assessment. The case study of alternative bread supply chains in France. *Journal of Cleaner Production*, *112*, 2452-2461.
21.	Lamnatou, C., Ezcurra-Ciaurriz, X., Chemisana, D., & Plà-Aragonés, L. M. (2016). Environmental assessment of a pork-production system in North-East of Spain focusing on life-cycle swine nutrition. *Journal of Cleaner Production*, *137*, 105-115.
22.	Lehuger, S., Gabrielle, B., & Gagnaire, N. (2009). Environmental impact of the substitution of imported soybean meal with locally-produced rapeseed meal in dairy cow feed. *Journal of Cleaner Production*, *17*(6), 616-624.
23.	Llorach-Massana, P., Muñoz, P., Riera, M. R., Gabarrell, X., Rieradevall, J., Montero, J. I., & Villalba, G. (2017). N2O emissions from protected soilless crops for more precise food and urban agriculture life cycle assessments. *Journal of cleaner production*, *149*, 1118-1126.
24.	López-Andrés, J. J., Aguilar-Lasserre, A. A., Morales-Mendoza, L. F., Azzaro-Pantel, C., Pérez-Gallardo, J. R., & Rico-Contreras, J. O. (2018). Environmental impact assessment of chicken meat production via an integrated methodology based on LCA, simulation and genetic algorithms. *Journal of cleaner production*, *174*, 477-491.
25.	Markussen, M., Kulak, M., Smith, L., Nemecek, T., & Østergård, H. (2014). Evaluating the sustainability of a small-scale low-input organic vegetable supply system in the United Kingdom. *Sustainability*, *6*(4), 1913-1945.
26.	McAuliffe, G. A., Takahashi, T., & Lee, M. R. (2018). Framework for life cycle assessment of livestock production systems to account for the nutritional quality of final products. *Food and energy security*, *7*(3), e00143.
27.	McCarthy, D., Matopoulos, A., & Davies, P. (2015). Life cycle assessment in the food supply chain: a case study. *International Journal of Logistics Research and Applications*, *18*(2), 140-154.
28.	McDevitt, J. E., & Milà i Canals, L. (2011). Can life cycle assessment be used to evaluate plant breeding objectives to improve supply chain sustainability? A worked example using porridge oats from the UK. *International Journal of Agricultural Sustainability*, *9*(4), 484-494.
29.	Miah, J. H., Griffiths, A., McNeill, R., Halvorson, S., Schenker, U., Espinoza-Orias, N. D., ... & Sadhukhan, J. (2018). Environmental management of confectionery products: Life cycle impacts and improvement strategies. *Journal of cleaner production*, *177*, 732-751.
30.	Mouron, P., Willersinn, C., Möbius, S., & Lansche, J. (2016). Environmental profile of the Swiss supply chain for French fries: Effects of food loss reduction, loss treatments and process modifications. *Sustainability*, *8*(12), 1214.
31.	Neira, D. P., Montiel, M. S., Cabeza, M. D., & Reigada, A. (2018). Energy use and carbon footprint of the tomato production in heated multi-tunnel greenhouses in Almeria within an exporting agri-food system context. *Science of The Total Environment*, *628*, 1627-1636.

32.	Neto, B., Dias, A. C., & Machado, M. (2013). Life cycle assessment of the supply chain of a Portuguese wine: from viticulture to distribution. *The International Journal of Life Cycle Assessment*, *18*(3), 590-602.
33.	Notarnicola, B., Sala, S., Anton, A., McLaren, S. J., Saouter, E., & Sonesson, U. (2017). The role of life cycle assessment in supporting sustainable agri-food systems: A review of the challenges. *Journal of Cleaner Production*, *140*, 399-409.
34.	Noya, I., Aldea, X., González-García, S., Gasol, C. M., Moreira, M. T., Amores, M. J., ... & Boschmonart-Rives, J. (2017). Environmental assessment of the entire pork value chain in Catalonia–A strategy to work towards Circular Economy. *Science of the Total Environment*, *589*, 122-129.
35.	Noya, L. I., Vasilaki, V., Stojceska, V., Gonzalez-García, S., Kleynhans, C., Tassou, S., ... & Katsou, E. (2018). An environmental evaluation of food supply chain using life cycle assessment: A case study on gluten free biscuit products. *Journal of cleaner production*, *170*, 451-461.
36.	Palmieri, N., Forleo, M. B., & Salimei, E. (2017). Environmental impacts of a dairy cheese chain including whey feeding: an Italian case study. *Journal of Cleaner Production*, *140*, 881-889.
37.	Pattara, C., Raggi, A., & Cichelli, A. (2012). Life cycle assessment and carbon footprint in the wine supply-chain. *Environmental management*, *49*(6), 1247-1258.
38.	Pelletier, N. (2017). Life cycle assessment of Canadian egg products, with differentiation by hen housing system type. *Journal of Cleaner Production*, *152*, 167-180.
39.	Pelton, R. E., & Smith, T. M. (2015). Hotspot scenario analysis: Comparative streamlined LCA approaches for green supply chain and procurement decision making. *Journal of Industrial Ecology*, *19*(3), 427-440.
40.	Perez-Neira, D., & Grollmus-Venegas, A. (2018). Life-cycle energy assessment and carbon footprint of peri-urban horticulture. A comparative case study of local food systems in Spain. *Landscape and Urban Planning*, *172*, 60-68.
41.	Piezer, K., Petit-Boix, A., Sanjuan-Delmás, D., Briese, E., Celik, I., Rieradevall, J., ... & Apul, D. (2019). Ecological network analysis of growing tomatoes in an urban rooftop greenhouse. *Science of the Total Environment*, *651*, 1495-1504.
42.	Putman, B., Thoma, G., Burek, J., & Matlock, M. (2017). A retrospective analysis of the United States poultry industry: 1965 compared with 2010. *Agricultural systems*, *157*, 107-117.
43.	Recanati, F., Marveggio, D., & Dotelli, G. (2018). From beans to bar: A life cycle assessment towards sustainable chocolate supply chain. *Science of the Total Environment*, *613*, 1013-1023.
44.	Reckmann, K., & Krieter, J. (2015). Environmental impacts of the pork supply chain with regard to farm performance. *The Journal of Agricultural Science*, *153*(3), 411-421.
45.	Rivera, X. C. S., Orias, N. E., & Azapagic, A. (2014). Life cycle environmental impacts of convenience food: Comparison of ready and home-made meals. *Journal of cleaner production*, *73*, 294-309.
46.	Roy, P., Nei, D., Orikasa, T., Xu, Q., Okadome, H., Nakamura, N., & Shiina, T. (2009). A review of life cycle assessment (LCA) on some food products. *Journal of food engineering*, *90*(1), 1-10.
47.	Ruviaro, C. F., Gianezini, M., Brandão, F. S., Winck, C. A., & Dewes, H. (2012). Life cycle assessment in Brazilian agriculture facing worldwide trends. *Journal of Cleaner Production*, *28*, 9-24.
48.	Sacchi, R. (2018). A trade-based method for modelling supply markets in consequential LCA exemplified with Portland cement and bananas. *The International Journal of Life Cycle Assessment*, *23*(10), 1966-1980.
49.	Salomone, R., & Ioppolo, G. (2012). Environmental impacts of olive oil production: a Life Cycle Assessment case study in the province of Messina (Sicily). *Journal of cleaner production*, *28*, 88-100.
50.	Six, L., De Wilde, B., Vermeiren, F., Van Hemelryck, S., Vercaeren, M., Zamagni, A., ... & De Meester, S. (2017). Using the product environmental footprint for supply chain management: lessons learned from a case study on pork. *The International Journal of Life Cycle Assessment*, *22*(9), 1354-1372.
51.	Sonesson, U. G., Lorentzon, K., Andersson, A., Barr, U. K., Bertilsson, J., Borch, E., ... & Hamberg, L. (2016). Paths to a sustainable food sector: integrated design and LCA of future food supply chains: the case of pork production in Sweden. *The International Journal of Life Cycle Assessment*, *21*(5), 664-676.

52.	Stoessel, F., Juraske, R., Pfister, S., & Hellweg, S. (2012). Life cycle inventory and carbon and water FoodPrint of fruits and vegetables: Application to a Swiss retailer. *Environmental science & technology*, *46*(6), 3253-3262.
53.	Svanes, E., & Aronsson, A. K. (2013). Carbon footprint of a Cavendish banana supply chain. *The International Journal of Life Cycle Assessment*, *18*(8), 1450-1464.
54.	Tasca, A. L., Nessi, S., & Rigamonti, L. (2017). Environmental sustainability of agri-food supply chains: An LCA comparison between two alternative forms of production and distribution of endive in northern Italy. *Journal of Cleaner Production*, *140*, 725-741.
55.	Theurl, M. C., Haberl, H., Erb, K. H., & Lindenthal, T. (2014). Contrasted greenhouse gas emissions from local versus long-range tomato production. *Agronomy for sustainable development*, *34*(3), 593-602.
56.	Tsarouhas, P., Achillas, C., Aidonis, D., Folinas, D., & Maslis, V. (2015). Life Cycle Assessment of olive oil production in Greece. *Journal of cleaner production*, *93*, 75-83.
57.	Usva, K., Saarinen, M., & Katajajuuri, J. M. (2009). Supply chain integrated LCA approach to assess environmental impacts of food production in Finland. *Agricultural and Food Science*, *18*(3-4), 460-476.
58.	van Putten, I. E., Farmery, A. K., Green, B. S., Hobday, A. J., Lim-Camacho, L., Norman-López, A., & Parker, R. W. (2016). The environmental impact of two Australian rock lobster fishery supply chains under a changing climate. *Journal of Industrial Ecology*, *20*(6), 1384-1398.
59.	Webb, J., Williams, A. G., Hope, E., Evans, D., & Moorhouse, E. (2013). Do foods imported into the UK have a greater environmental impact than the same foods produced within the UK?. *The International Journal of Life Cycle Assessment*, *18*(7), 1325-1343.
60.	Wiedemann, S. G., Ledgard, S. F., Henry, B. K., Yan, M. J., Mao, N., & Russell, S. J. (2015). Application of life cycle assessment to sheep production systems: investigating co-production of wool and meat using case studies from major global producers. *The International Journal of Life Cycle Assessment*, *20*(4), 463-476.
61.	Wiedemann, S. G., McGahan, E. J., & Murphy, C. M. (2017). Resource use and environmental impacts from Australian chicken meat production. *Journal of Cleaner Production*, *140*, 675-684.
62.	Wiedemann, S., McGahan, E., Murphy, C., Yan, M. J., Henry, B., Thoma, G., & Ledgard, S. (2015). Environmental impacts and resource use of Australian beef and lamb exported to the USA determined using life cycle assessment. *Journal of Cleaner Production*, *94*, 67-75.
63.	Wikström, F., Williams, H., Verghese, K., & Clune, S. (2014). The influence of packaging attributes on consumer behaviour in food-packaging life cycle assessment studies-a neglected topic. *Journal of Cleaner Production*, *73*, 100-108.
64.	Xiao, X., Zhu, Z., Fu, Z., Mu, W., & Zhang, X. (2018). Carbon Footprint Constrained Profit Maximization of Table Grapes Cold Chain. *Agronomy*, *8*(7), 125.
65.	Zhao, R., Xu, Y., Wen, X., Zhang, N., & Cai, J. (2018). Carbon footprint assessment for a local branded pure milk product: a lifecycle based approach. *Food Science and Technology*, *38*(1), 98-105.
66.	Ziegler, F., Hornborg, S., Green, B. S., Eigaard, O. R., Farmery, A. K., Hammar, L., ... & Vázquez-Rowe, I. (2016). Expanding the concept of sustainable seafood using Life Cycle Assessment. *Fish and Fisheries*, *17*(4), 1073-1093.

JET Journal of Energy Technology

Author instructions

www.fe.um.si/en/jet.html

MAIN TITLE OF THE PAPER
SLOVENIAN TITLE

*Author[1], Author [2], Corresponding author*ℜ

Keywords: (Up to 10 keywords)

Abstract

Abstract should be up to 500 words long, with no pictures, photos, equations, tables, only text.

Povzetek

(Abstract in Slovenian language)

Submission of Manuscripts: All manuscripts must be submitted in English by e-mail to the editorial office at jet@um.si to ensure fast processing. Instructions for authors are also available online at http://www.fe.um.si/en/jet/author-instructions.html.

Preparation of manuscripts: Manuscripts must be typed in English in prescribed journal form (MS Word editor). A MS Word template is available at the Journal Home page.

A title page consists of the main title in the English and Slovenian language; the author(s) name(s) as well as the address, affiliation, E-mail address, telephone and fax numbers of author(s). Corresponding author must be indicated.

Main title: should be centred and written with capital letters (ARIAL bold 18 pt), in first paragraph in English language, in second paragraph in Slovenian language.

Key words: A list of 3 up to 6 key words is essential for indexing purposes. (CALIBRI 10pt)

Abstract: Abstract should be up to 500 words long, with no pictures, photos, equations, tables, - text only.

Povzetek: - Abstract in Slovenian language.

Main text should be structured logically in chapters, sections and sub-sections. Type of letters is Calibri, 10pt, full justified.

ℜ Corresponding author: Title, Name and Surname, Organisation, Department, Address, Tel.: +XXX x xxx xxx, E-mail address: x.x@xxx.xx

[1] Organisation, Department, Address

[2] Organisation, Department, Address

Units and abbreviations: Required are SI units. Abbreviations must be given in text when first mentioned.

Proofreading: The proof will be send by e-mail to the corresponding author in MS Word's Track changes function. Corresponding author is required to make their proof corrections with accepting or rejecting the tracked changes in document and answer all open comments of proof reader. The corresponding author is responsible to introduce corrections of data in the paper. The Editors are not responsible for damage or loss of submitted text. Contributors are advised to keep copies of their texts, illustrations and all other materials.

The statements, opinions and data contained in this publication are solely those of the individual authors and not of the publisher and the Editors. Neither the publisher nor the Editors can accept any legal responsibility for errors that could appear during the process.

Copyright: Submissions of a publication article implies transfer of the copyright from the author(s) to the publisher upon acceptance of the paper. Accepted papers become the permanent property of "Journal of Energy Technology". All articles published in this journal are protected by copyright, which covers the exclusive rights to reproduce and distribute the article as well as all translation rights. No material can be published without written permission of the publisher.

Chapter examples:

1 MAIN CHAPTER

(Arial bold, 12pt, after paragraph 6pt space)

1.1 Section

(Arial bold, 11pt, after paragraph 6pt space)

1.1.1 Sub-section

(Arial bold, 10pt, after paragraph 6pt space)

Example of Equation (lined 2 cm from left margin, equation number in normal brackets (section. equation number), lined right margin, paragraph space 6pt before in after line):

Equation (1.1)

Tables should have a legend that includes the title of the table at the top of the table. Each table should be cited in the text.

Table legend example:

Table 1: *Name of the table (centred, on top of the table)*

Figures and images should be labelled sequentially numbered (Arabic numbers) and cited in the text – Fig.1 or Figure 1. The legend should be below the image, picture, photo or drawing.

Figure legend example:

Figure 1: *Name of the figure (centred, on bottom of figure, photo, or drawing)*

References

[1] **N. Surname:** *Title,* Journal Title, Vol., Iss., p.p., Year of Publication

[2] **N. Surname:** *Title,* Publisher, Year of Publication

[3] **N. Surname:** *Title* [online], Publisher or Journal Title, Vol., Iss., p.p., Year of Publication. Available: website (date accessed)

Examples:

[1] **J. Usenik**: *Mathematical model of the power supply system control*, Journal of Energy Technology, Vol. 2, Iss. 3, p.p. 29 – 46, 2009

[2] **J. J. DiStefano, A.R. Stubberud, I. J. Williams**: *Theory and Problems of Feedback and Control Systems*, McGraw-Hill Book Company, 1987

[3] **T. Žagar, L. Kegel:** *Preparation of National programme for SF and RW management taking into account the possible future evolution of ERDO* [online], Journal of Energy Technology, Vol. 9, Iss. 1, p.p. 39 – 50, 2016. Available: http://www.fe.um.si/images/jet /Volume 9_Issue1/03-JET_marec_2016-PREPARATION_OF_NATIONAL.pdf (7. 10. 2016)

Example of reference-1 citation: In text *[1],* text continue.

Nomenclature

(Symbols)	(Symbol meaning)
t	time

JET

JET I Journal of Energy Technology I Vol. 12, Issue 1, April 2019 I University of Maribor, Faculty of Energy Technology

ISSN 1855-5748

9 771855 574008